Universidade de Aveiro Departamento de Química
2018

Pedro Gonçalo Simões Vieira

Produção de extratos bioativos a partir de resíduos de *Quercus cerris* por extração supercrítica com solventes verdes

Universidade de Aveiro Departamento de Química
2018

Pedro Gonçalo Simões Vieira

Produção de extratos bioativos a partir de resíduos de *Quercus cerris* por extração supercrítica com solventes verdes

Dissertação apresentada à Universidade de Aveiro para cumprimento dos requisitos necessários à obtenção do grau de Mestre em Engenharia Química, realizada sob a orientação científica do Doutor Carlos Manuel Silva, Professor Associado do Departamento de Química da Universidade de Aveiro, e coorientação do Doutor Marcelo Melo, investigador de pós-doutoramento do Departamento de Química da Universidade de Aveiro

Dedico este trabalho aos meus pais por todo o apoio e incentivo.

o júri

presidente

Professora Doutora Maria Inês Purcell de Portugal Branco
Professora Auxiliar do Departamento de Química da Universidade de Aveiro

Doutor António Augusto Areosa Martins
Investigador de Pós-Doutoramento no Laboratório de Engenharia de Processos, Ambiente, Biotecnologia e Energia da Faculdade de Engenharia da Universidade do Porto

Professor Doutor Carlos Manuel Santos da Silva
Professor Associado do Departamento de Química da Universidade de Aveiro

agradecimentos

Agradeço ao Professor Doutor Carlos Manuel Silva pela oportunidade que me deu, pela amizade, pela disponibilidade e pelos ensinamentos transmitidos ao longo dos cincos anos do curso.
Ao Doutor Marcelo Melo, pelo apoio laboratorial e na construção do documento e por todo o conhecimento que me transmitiu durante toda a dissertação.
À Professora Inês Portugal e ao Professor Mário Simões pela disponibilidade e colaboração.
Aos colegas do grupo EgiChem, pelas horas de companhia no laboratório e no gabinete, pelas importantes discussões e por todos os contributos.
Aos meus amigos mais próximos, pelo apoio que me deram durante toda esta jornada e pela força que sempre me transmitiram; aqui faço também uma referência especial a todos aqueles que comigo trabalharam durante os três anos de NEEQu-AAUAv e que tanto contribuíram para ser a pessoa que sou hoje.
À Inês, por ser a namorada fantástica que é, por estar sempre ao meu lado, pela paciência de me ouvir falar de coisas que nem sabe o que são e pelas palavras que sempre teve para me dizer.
À minha irmã e aos meus pais, pelo esforço que fizeram e fazem para permitirem que concretizasse o sonho de tirar um curso superior na Universidade da minha cidade, por sempre terem acreditado em mim e pelos valores que sempre me transmitiram.

palavras-chave

Cortiça, cossolvente, extração supercrítica, fridelina, otimização, *Quercus cerris*, seletividade

resumo

Esta dissertação teve como objetivo estudar a produção e caracterização de extratos ricos em compostos bioativos (nomeadamente fridelina) a partir de cortiça de *Quercus cerris*. Realizaram-se extrações Soxhlet e extrações sólido-líquido (SLE) em descontínuo com metanol, etanol, diclorometano e éter de petróleo, assim como extração supercrítica (SFE) com dióxido de carbono modificado (por adição de etanol). Os extratos produzidos foram caracterizados por FTIR-ATR e GC-MS e o método de escalonamento multidimensional (MDS) foi aplicado para comparação dos mesmos. Realizou-se uma otimização experimental de SFE, usando um desenho fatorial de experiências do tipo Box-Behnken e a metodologia de superfícies de resposta.

O rendimento total de extração (η_{Total}) máximo foi obtido para o ensaio Soxhlet com metanol (η_{Total} = 13.8 wt.%) e o rendimento mínimo foi obtido para extração sólido-líquido em descontínuo com éter de petróleo (η_{Total} = 0.35 wt.%). Registou-se uma variabilidade significativa dos valores de η_{Total}, marcada pelos rendimentos superiores para extração com solventes polares, nomeadamente metanol e etanol. No caso da extração supercrítica, η_{Total} variou de 1.2 wt.% no ensaio SFE3 (50 ℃, 2.5 wt.% EtOH, 5 $\mathrm{g\,min^{-1}}$) até 1.7 wt.% no ensaio SFE4 (60 ℃, 2.5 wt.% EtOH, 8 $\mathrm{g\,min^{-1}}$). Em termos de concentração em fridelina ($C_{\mathrm{Friedelin}}$), os resultados oscilaram entre 41.3 wt. % (Soxhlet com diclorometano) e 5.4 wt. % (SLE em descontínuo com éter de petróleo). Os melhores resultados em termos de $C_{\mathrm{Friedelin}}$ foram os que envolveram solventes pouco polares/apolares. Os ensaios SFE atingiram resultados de $C_{\mathrm{Friedelin}}$ melhores do que a maioria dos ensaios de extração Soxhlet e sólido-líquido em descontínuo, o que confirma a interessante seletividade do processo para a fridelina. A análise MDS destacou a maior proximidade química entre os extratos alcoólicos e a biomassa, e entre os extratos de solventes apolares ou pouco polares e a fridelina pura.

Para a otimização experimental de SFE da cortiça *Q. cerris*, as condições que maximizam η_{Total} (2.2 wt.%) e $\alpha_{\mathrm{F,nF}}$ (3.3 para t = 8.0 h) são valores máximos de T (60 ℃), teor de etanol (5 wt.%) e de caudal de CO_2 (11 $\mathrm{g\,min^{-1}}$). De registar os valores de seletividade superior a 1.0 no espaço experimental estudado, o que confirma que a fridelina é removida seletivamente por SFE. No caso de $C_{\mathrm{Friedelin}}$, o valor máximo (38.2 wt.%) foi obtido para a combinação de baixa temperatura (40 ℃), ausência de cossolvente (0 wt.% EtOH) e menor caudal (5 $\mathrm{g\,min^{-1}}$). Em definitivo, as condições ótimas dependerão de qual o principal objetivo da extração: um extrato rico numa maior diversidade de compostos (maior η_{Total}) ou em compostos alvo como a fridelina (maior $C_{\mathrm{Friedelin}}$).

No geral, este trabalho fornece argumentos importantes para a produção de extratos ricos em fridelina a partir da cortiça de *Quercus cerris,* através da tecnologia SFE no âmbito do conceito de biorrefinaria.

keywords

Cork, cosolvent, friedelin, optimization, *Quercus cerris*, selectivity, supercritical fluid extraction

abstract

The present work studied the production and characterization of extracts rich in bioactive compounds (namely friedelin) from *Quercus cerris* cork. Soxhlet and batch solid-liquid extraction (SLE) with methanol, ethanol, dichloromethane and petroleum ether were carried out, as well as supercritical fluid extraction (SFE) using modified carbon dioxide (by addition of ethanol). The produced extracts were characterized by FTIR-ATR and GC-MS, and multidimensional scaling (MDS) was applied to compare them. The optimization of SFE was performed using Box-Behnken design of experiments and response surface methodology.

The maximum total extraction yield (η_{Total}) was attained for the Soxhlet extraction with methanol (η_{Total} = 13.8 wt.%) and the minimum was attained in batch SLE with petroleum ether (η_{Total} = 0.35 wt.%). A significant variability of η_{Total} values was evident, marked by the higher yields obtained with polar solvents, namely methanol and ethanol. For the supercritical fluid extractions, η_{Total} ranged from 1.2 wt.% for run SFE3 (50 ℃, 2.5 wt.% EtOH, 5 $\mathrm{g\,min^{-1}}$) to 1.7 wt.% for run SFE4 (60 ℃, 2.5 wt.% EtOH, 8 $\mathrm{g\,min^{-1}}$). For friedelin concentration ($C_{\mathrm{Friedelin}}$), the results ranged from 41.3 wt.% (Soxhlet with dichloromethane) to 5.4 wt.% (batch SLE with methanol). The best performing assays on $C_{\mathrm{Friedelin}}$ were those involving weakly polar/non-polar solvents. The SFE assays provided $C_{\mathrm{Friedelin}}$ results better than most Soxhlet and batch SLE experiments, which confirms the interesting selectivity to friedelin ($\alpha_{\mathrm{F,nF}}$). MDS analysis highlighted the chemical proximity between the alcoholic extracts and the biomass, and between the weakly or non-polar solvent extracts and pure friedelin.

For the experimental optimization of SFE of *Q. cerris* cork, the conditions that maximize η_{Total} (2.2 wt.%) and $\alpha_{\mathrm{F,nF}}$ (3.3 at t = 8.0 h) were the maximum values of T (60 ℃), ethanol content (5 wt.%) and CO_2 flow rate (11 $\mathrm{g\,min^{-1}}$). In fact, the selectivity values were higher than 1.0 anywhere within the studied experimental space, which shows that friedelin can be removed selectively over all the other compounds by SFE. For friedelin concentration, the maximum ($C_{\mathrm{Friedelin}}$= 38.2 wt.%) was attained for the combination of a lower temperature (40 ℃), no cosolvent (0 wt.% EtOH) and lower CO_2 flow rate (5 $\mathrm{g\,min^{-1}}$). The optimal conditions depend on what is the main goal of extraction: an extract enriched in a higher diversity of compounds (higher η_{Total}) or in a target compound like friedelin (higher $C_{\mathrm{Friedelin}}$).

On the whole, this work provides strong arguments towards the production of friedelin enriched extracts from *Quercus cerris* cork through SFE technology, under the biorefinery concept.

Index

Figures list ii
Tables list iv
I. Motivation and structure of the thesis 1
II. Publication 1 4
1. Introduction 5
2. Materials and methods 7
2.1 Chemicals and biomass samples 7
2.2 Soxhlet extraction 8
2.3 Batch solid-liquid extraction 8
2.4 Supercritical fluid extraction 8
2.5 Fourier Transform Infrared-Attenuated Total Reflectance (FTIR-ATR) spectroscopy analysis 9
2.6 Gas Chromatography Mass Spectroscopy (GC-MS) analysis 10
2.7 Multidimensional scaling analysis 11
3. Results and discussion 12
3.1 Characterization of full extracts 12
3.1.1 Total extraction yield 12
3.1.2 Volatile extractives: friedelin yield and concentration 13
3.1.3 FTIR-ATR results 15
3.2 Multidimensional scaling analysis 18
4. Conclusions 23
5. References 24
III. Publication 2 31
1. Introduction 32
2. Materials and methods 34
2.1 Chemicals and biomass samples 34
2.2 Extraction processes 34
2.3 Design of Experiments and Response Surface Methodology (DoE/RSM) 36
2.4 Gas Chromatography Mass Spectroscopy (GC-MS) analysis 37
3. Results and discussion 38
3.1 Experimental optimization of the SFE operating conditions 38
3.1.1 Total extraction yield 43
3.1.2 Friedelin concentration 44
3.1.3 Selectivity to friedelin 45
3.2 Experiments at optimal operating conditions 46
3.3 Validation tests 49
4. Conclusions 52
5. References 53
IV. Final conclusions and future work 57

Figures list

Publication 1

Figure 1 – (a) Molecular structure of the target compound friedelin and (b) Quercus cerris cork of 20-40 mesh particle size.

Figure 2 – Simplified flowsheet of the SFE unit of this work.

Figure 3 – Illustrative comparison of the total extraction yields from *Q. cerris* cork (20-40 mesh) obtained with different extractions methods and solvents. See Table 1 for experimental conditions.

Figure 4 – GC-MS chromatogram of Soxhlet dichloromethane extract of Q. cerris cork.

Figure 5 - FTIR-ATR spectra of Soxhlet, batch SLE and supercritical extracts, of original biomass sample and pure friedelin.

Figure 6 - MDS maps of: (a) FTIR-ATR, (b) GC-MS and (c) both FTIR-ATRT and GC-MS.

Publication 2

Figure 1 – Simplified flowsheet of the SFE unit of this work.

Figure 2 – Pareto charts for the supercritical fluid extraction of Q. cerris cork, showing the influence of factors on the (a) total extraction yield (η_{Total}), (b) friedelin concentration in the extract ($C_{\mathrm{Friedelin}}$), and (c) selectivity towards friedelin ($\alpha_{\mathrm{F,nF}}$).

Figure 3 – Response surfaces plotting the effects of (a) temperature and carbon dioxide flow rate on total extraction yield, for 5 wt.% EtOH content, and (b) ethanol content and carbon dioxide flow rate on total extraction yield, at 50 ℃ . Dots are experimental data and response surfaces are given by Eq. (10).

Figure 4 - Response surface plotting the effects of (a) temperature and carbon dioxide flow rate on friedelin concentration for 5 wt.% EtOH content and (b) ethanol content and carbon dioxide flow rate friedelin concentration at 50℃ (reduced model). Dots are experimental data and surface response is given by Eq. (11).

Figure 5 - Response surface plotting the effects of (a) temperature and carbon dioxide flow rate on selectivity to friedelin for 5 wt.% EtOH content and (b) ethanol content and carbon dioxide flow rate on selectivity to friedelin at 50 ℃ (reduced model). Dots are experimental data and surface is given by Eq. (12).

Figure 6 – Experimental total extraction yield for predicted optimum operating conditions (SFE16), and for an additional assays with 20 wt.% of EtOH. Data from the

original Box-Behnken design plan (SFE11 and SFE15) are plotted for comparison.
Figure 7 - Experimental friedelin concentration for predicted optimum operating conditions (SFE16), and for an additional assays with 20 wt.% of EtOH. Data from the original Box-Behnken design plan (SFE11 and SFE15) are plotted for comparison.
Figure 8 – Predicted versus measured total extraction yield (wt.%) for the Design of Experiments (DoE) and validation tests.

Tables list

Publication 1

Table 1 – Experimental conditions for the extraction assays carried out.

Table 2 – Friedelin extraction yield and friedelin concentration of the Soxhlet, batch SLE and supercritical extractions.

Table 3 – Compilation of the selected FTIR-ATR spectra peaks (in wavenumber units) and the associated chemical and GC-MS peaks (in retention time units) with the corresponding compound for the MDS analysis.

Table 4 - Stress values for the scale reduction of FTIR-ATR and GC-MS multidimensional data.

Publication 2

Table 1 - Correspondence of the different levels and factors considered in codified and non-codified format.

Table 2 – Experimental conditions and results of the extraction assays carried out in this work. Pressure, particle size and extraction time were held constant at 300 bar, 20-40 mesh and 8 h, respectively.

Table 3 – Regression coefficients of the RSM polynomial given by Eq. (7), their individual significance at 90 %/95% confidence level and respective determination coefficients for the full model (FM); values in bold represents significant coefficients.

Table 4 – Reduced experimental models (RM) fitted to the responses listed in Table 2.

Table 5 - Optimum conditions for each response and predicted response values under these conditions.

Table 6 – Experimental results from previous chapter and from literature and predicted results for model validation.

I. Motivation and structure of the thesis

During the last years, science and technology have focused on the development of new integrated use of biomass through its conversion into useful products under the biorefinery paradigm, by which the biomass value is maximized through physicochemical and/or biological unit operations and processes.

Within the several pathways on course for biorefinery, the production of extracts from vegetable matrices has gained high interest due the richness of bioactive and functional compounds found in natural biomasses, which can thus be explored for vast applications, including food, nutraceutical, cosmetics or pharmacological fields [1][2]. For instance, the use of natural compounds for preserving quality of products [3] and/or as green corrosion inhibitor [4] are two examples of application under research. In this context, the great challenge nowadays in the natural extracts research has been the production of safe and high quality extracts/products, preferably using innocuous solvents and reducing energy consumption, i.e. under the *green extraction* concept [5].

In this general context, the interest around cork based products has been equally increasing due the specific natural properties of this raw material, and the multitude of different industrial applications where it can be applied. In turn, the latter produce large amounts of by-products (cork powder). The world cork production reached 201 thousand tons in 2010, of which Portugal is the production leader with almost 50 % of world production [6]. Cork oak (*Quercus suber L.*) is one of the most dominant forest species in Portugal [6] and it is characterized by the presence of a thick and rugged bark with a continuous layer of cork in its outer part [7]. The cork stoppers are the most important product of cork industry followed by other applications such as insulation and surfacing materials [7].

On the other hand, in Easter Europe and Minor Asia another *Quercus* species prevails [8][9]: *Quercus cerris.* Its bark is rich in cork and has been explored for nothing more than its suitability as fuel. In turn, in recent years there has been an increasing interest to valorize the cork of this species, namely through its occurring extractives [9]–[11]. The molecules that compose the cork extractive fraction are typically divided in two main groups: phenolic compounds, most efficiently obtained with polar solvents (such as water, methanol and ethanol), and aliphatic and terpenoid

compounds, better extracted using non-polar or weakly polar solvents (such as dichloromethane, n-hexane, or supercritical CO_2) [12].

Accordingly, supercritical fluid extraction (SFE) is one of the most recognized technologies for the extraction of vegetables matrices, which has been developed since de 1970s. The most widely used solvent for SFE is carbon dioxide (SC-CO_2) that evidences a solvent power comparable to typical organic solvents. Moreover, SC-CO_2 also favors high diffusivities, low viscosity, null surface tension, and a simple recovery process with solvent-free products. The extraction processes involving SC-CO_2 can run at moderate temperatures, which prevents thermal degradation of some compounds in extracts [2]. The low critical proprieties of CO_2 also allows an easy separation from the sample.

The present work aims at the production and characterization of extracts from *Quercus cerris* cork. For this the application of different extraction methods (batch solid-liquid extraction, Soxhlet extraction, and SFE) and solvents with different polarity was targeted. In particular, the optimization of friedelin production through supercritical fluid extraction was addressed in more detail, standing thus as an important contribution of the thesis. Accordingly, the performed work allowed a comparison between the different extraction methods, a detailed characterization of the produced *Q. cerris* cork extracts, and the appraisal of solvent polarity influence in the quality of extracts and their resemblance with the original vegetal matrix.

The thesis work was structured to originate two scientific publications, which constitute the two major chapters of this document. They are:

Publication 1 [13]**:** "*Quercus cerris* extracts obtained by distinct separation methods and solvents, and detailed characterization by chemical similarity analysis."

Publication 2 [14]: "Optimization of the supercritical fluid extraction of *Quercus cerris* cork: Influence of operating conditions in total extraction yield, friedelin concentration and selectivity."

References

[1] R. P. F. F. da Silva, T. A. P. Rocha-Santos, and A. C. Duarte, "Supercritical fluid extraction of bioactive compounds," *TrAC - Trends Anal. Chem.*, vol. 76, pp. 40–51, 2016.

[2] M. M. R. De Melo, A. J. D. Silvestre, and C. M. Silva, "Supercritical fluid extraction of vegetable matrices: Applications, trends and future perspectives of a convincing green technology," *J. Supercrit. Fluids*, vol. 92, pp. 115–176, 2014.

[3] N. Chatrabnous, N. Yazdani, V. Tavallali, and K. Vahdati, "Preserving quality of fresh walnuts using plant extracts," *LWT - Food Sci. Technol.*, vol. 91, no. January, pp. 1–7, 2018.

[4] P. E. Alvarez, M. V. Fiori-Bimbi, A. Neske, S. A. Brandán, and C. A. Gervasi, "Rollinia occidentalis extract as green corrosion inhibitor for carbon steel in HCl solution," *J. Ind. Eng. Chem.*, vol. 58, pp. 92–99, 2018.

[5] F. Chemat, M. A. Vian, and G. Cravotto, "Green Extraction of Natural Products: Concept and Principles," *Int. J. Mol. Sci.*, vol. 13, no. 7, pp. 8615–8627, Jul. 2012.

[6] APCOR, "CORTIÇA | CORK 2017/2018."

[7] H. Pereira, *Cork: Biology, Production and Uses*. 2007.

[8] A. Şen, T. Quilho, and H. Pereira, "Bark anatomy of Quercus cerris L. var. cerris from Turkey," *Turk. J. Botany*, vol. 35, pp. 45–55, 2011.

[9] A. Şen, I. Miranda, S. Santos, J. Graça, and H. Pereira, "The chemical composition of cork and phloem in the rhytidome of Quercus cerris bark," *Ind. Crops Prod.*, vol. 31, no. 2, pp. 417–422, 2010.

[10] A. Şen, M. M. R. De Melo, A. J. D. Silvestre, H. Pereira, and C. M. Silva, "Prospective pathway for a green and enhanced friedelin production through supercritical fluid extraction of Quercus cerris cork," *J. Supercrit. Fluids*, vol. 97, pp. 247–255, 2015.

[11] M. M. R. de Melo, A. Şen, A. J. D. Silvestre, H. Pereira, and C. M. Silva, "Experimental and modeling study of supercritical CO2 extraction of Quercus cerris cork: Influence of ethanol and particle size on extraction kinetics and selectivity to friedelin," *Sep. Purif. Technol.*, vol. 187, pp. 34–45, 2017.

[12] I. M. Aroso, A. R. Araújo, R. A. Pires, and R. L. Reis, "Cork: Current Technological Developments and Future Perspectives for this Natural, Renewable, and Sustainable Material," *ACS Sustain. Chem. Eng.*, vol. 5, no. 12, pp. 11130–11146, 2017.

[13] P. G. Vieira *et al.*, "*Quercus cerris* extracts obtained by distinct separation methods and solvents, and detailed characterization by chemical similarity analysis," 2018.

[14] P. G. Vieira *et al.*, "Optimization of the supercritical fluid extraction of Quercus cerris cork. Influence of operating conditions in total extraction yield, friedelin concentration and selectivity," 2018.

II. Publication 1

Quercus cerris extracts obtained by distinct separation methods and solvents, and detailed characterization by chemical similarity analysis

Pedro G. Vieira[1], Marcelo M.R. de Melo[1], Ali Şen[2], Mário M.Q. Simões[3], Inês Portugal[1], Helena Pereira[2], Carlos M. Silva[1]*

[1] CICECO – Aveiro Institute of Materials, Department of Chemistry, University of Aveiro, Aveiro 3810-193, Portugal

[2] Centro de Estudos Florestais, Instituto Superior de Agronomia, Universidade de Lisboa, Tapada da Ajuda, 1349-017 Lisboa, Portugal

[3] QOPNA, Department of Chemistry, University of Aveiro, Aveiro, Portugal

Keywords:

Batch, Cork, *Quercus cerris*, Soxhlet, Supercritical, Multidimensional scaling

1. Introduction

In a changing world, the pursuit of sustainability has gained an increased importance and, in this respect, the environmental side effects of industrial processes are key phenomena to take into consideration. Accordingly, in many science and technology areas, scientists have been focusing on alternatives to their classical approaches. In this context, *Green Extraction* is based on the discovery and design of new extraction processes intended to reduce energy consumption, using less harmful solvents and ensuring a safe and high quality extract/product [1]. Recent trends in extraction techniques have largely focused on minimizing the use of organic solvents while allowing a cost-effective production of extracts [2].

Within the context of the extraction of natural products, the classical industrial approach has relied on batch solid-liquid extraction (SLE) using organic solvents (e.g. ethanol, methanol and *n*-hexane). Here, the biomass is immersed in the solvent and the extract is progressively solubilized until equilibrium is reached (or stopped before it). In turn, at lab level, Soxhlet extraction operates in crosscurrent mode (instead of batch) and stands as an established reference SLE technique. Since Soxhlet extraction is typically performed for extended periods of time (i.e. high number of extraction cycles) to exhaust the biomass, the results obtained through this method can be taken as comparison basis for alternative extraction processes [3]. Nevertheless, SLE methods are becoming controversial not only due to the use of organic solvents but also because at the end of the process the solvent still needs to be separated from the solid matrix and/or from the resulting extract (which imply environmental problems and high costs related to the elimination of the used solvent [3][4]). In this respect, some approaches to improve SLE have encompassed efficiency enhancement of these classical processes upon combination with microwaves [5], ultrasounds [6], or electrical fields and charges [7]. However, these strategies are not able to solve all of the identified sustainability drawbacks of SLE techniques.

On the other hand, two of the most sound alternative techniques for the extraction of vegetable matrices are supercritical fluid extraction (SFE) [8] and ionic liquids (ILs) extraction [9]. These two approaches allow an operational tuning of conditions towards an enhanced affinity to target bioactive compounds, which enable recoveries similar or better than the classical approaches. Moreover, both SFE and ILs extraction can ensure an innocuous impact to human health and to the environment,

namely if CO_2 is used for SFE and/or natural deep eutectic solvents (NADES) for ILs extraction. Nevertheless, only SFE allows a free-of-solvent extract at the end of the process, which is a valuable advantage over ILs and SLE. The two alternative methods have been researched in recent years either to extract edible oils from palm, sunflower and other vegetal sources [10]-[13], or valuable bioactive compounds from plants or waste residues, such as orange peels [14], eucalyptus leaves [15] and grape seed [16].

Among the plethora of biomass matrices available, cork is one interesting natural material not only because it is periodically renewed in some *Quercus* spp. trees, but also due to the important properties such as low permeability, biological inertia, hydrophobic behaviour and elastic compression [17][18]. Turkey oak (*Quercus cerris*) presents a cork outer shell, but it has been preferably used as fuel so far. Hence, under the biorefinery concept, an increased interest on the valorization of *Q. cerris* cork has been identified [18]–[23]. This includes the interest in bioactive compounds present in cork, namely friedelin, a pentacyclic triterpene ketone that has been shown to exhibit anti-tumor [24], anti-inflammatory [25], analgesic [25] and antipyretic [25] activities.

Since extracts from vegetal products typically include a high diversity of analytes with varying chemical natures, selective and sensitive analytical methods are necessary for their characterization. Among these are techniques such as High-Performance Liquid Chromatography (HPLC), Gas Chromatography coupled to Mass Spectroscopy (GC-MS), Fourier Transform Infrared spectroscopy with Attenuated Total Reflectance (FTIR-ATR) and Differential Scanning Calorimetry (DSC) [8][26]–[28]. While FTIR-ATR and DSC can provide general information on the full extract composition from the perspective of chemical bonds/groups (FTIR-ATR) or thermal profiles (DSC), GC-MS and HPLC are useful for the individual detection and rigorous quantification of volatile and heavy compounds, respectively. In this sense, the combination of analytical results opens the way to a more thorough appraisal of the chemical composition of the extracts obtained by different extractions methods and solvents. Moreover, these analytical data can be jointly processed and digested with chemometric techniques, namely multivariate statistic tools such as principal component analysis (PCA) [29], discriminant analysis (DA) [30], clusters analysis (CA) [15] and multidimensional scaling (MDS) [31].

In this study, five solvents (ethanol, methanol, petroleum ether and supercritical carbon dioxide) and three extraction methods (Soxhlet, batch SLE, and SFE) were applied to produce extracts from *Q. cerris* cork. The extracts from the different

processes were analysed regarding total extraction yield and friedelin content. GC-MS and FTIR-ATR were used as analytical methods, and MDS technique was used to establish proximity relations between the different extraction methods and solvents.

2. Materials and methods

2.1 Chemicals and biomass samples

CO_2 (purity 99 %) was supplied by Air Liquide (Algés, Portugal). Ethanol (purity 99.5 %) and dichloromethane (purity, 99.98%) were supplied by Fisher Scientific (Leicestershire, United Kingdom). Pyridine (purity 99.5 %), N,O-Bis(trimethylsilyl)trifluoroacetamine (BTSFA, purity 98 %), chlorotrimethylsilane (TMSCl, purity 99 %), friedelin (purity 95 %, see Figure 1a), methanol (purity 99 %) and tetracosane (purity 99 %) were supplied by Sigma Aldrich (Deutschland). Petroleum ether (purity 99%) was supplied by Chem-Lab NV (Zedelgem, Belgium).

Q. cerris bark was obtained from Kahramanmaras, Turkey, and was granulated with a hammer-type industrial mill (see Figure 1b). The resulting granules were separated by density difference in distilled water in 10 minutes mixing time. The floating fraction of cork-enriched granules (subsequently named cork) was dried and grinded into 20-40 mesh (0.42-0.84 mm), which is a trade-off particle size that minimizes the industrial milling effort according to a previous study [23]. The moisture content of the biomass was experimentally measured by drying *ca.* 3 g of cork at 60 ℃ for 24h. The sample was weighed before and after drying, being the moisture 5.6 wt.%.

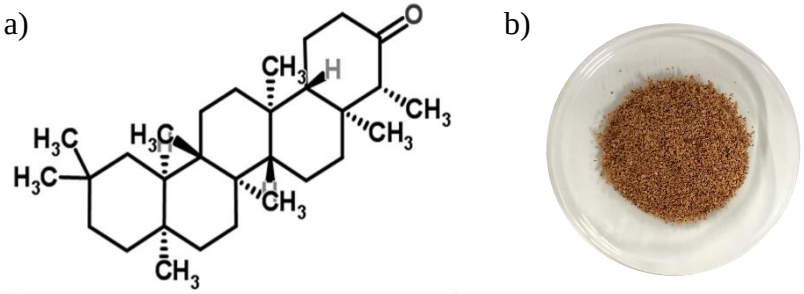

Figure 1 – (a) Molecular structure of the target compound friedelin and (b) *Quercus cerris* cork of 20-40 mesh particle size.

Total extraction yield (η_{Total}), friedelin extraction yield ($\eta_{\mathrm{Friedelin}}$) and friedelin concentration ($C_{\mathrm{Friedelin}}$) were calculated according to the following relations:

$$\eta_{\mathrm{Total}}(\mathrm{wt.\,\%}) = \frac{w_{\mathrm{extract}}}{w_{\mathrm{biomass}}} \times 100 \quad (1)$$

$$\eta_{\mathrm{Friedelin}}(\mathrm{wt.\,\%}) = \frac{w_{\mathrm{Friedelin}}}{w_{\mathrm{biomass}}} \times 100 \quad (2)$$

$$C_{\mathrm{Friedelin}}(\mathrm{wt.\,\%}) = \frac{w_{\mathrm{Friedelin}}}{w_{\mathrm{extract}}} \times 100 \quad (3)$$

where w_{extract} is the mass of dry extract, $w_{\mathrm{biomass}}$is the mass of dried cork used in the experiment, and $w_{\mathrm{friedelin}}$is the mass of friedelin quantified by GC-MS analysis of the extract.

2.2 Soxhlet extraction

Soxhlet extractions were carried out during 8 h, using *ca.* 3 g of 20-40 mesh *Q. cerris* cork and 120 mL of solvent. Four different solvents, namely methanol (S1), ethanol (S2), dichloromethane (S3) and petroleum ether (S4) were studied in order to evaluate the influence of solvent polarity in total extraction yield and friedelin concentration. The extracts samples of each run were evaporated, weighed and analysed by FTIR-ATR and GC-MS.

2.3 Batch solid-liquid extraction

Cork (*ca*. 3 g) was extracted individually with each of the four different organic solvents (30 mL) in a 1:10 w/v ratio. The extractions occurred in sealed and periodically manually shaken beakers for 24 h. The solvents used were methanol (B1), ethanol (B2), dichloromethane (B3) and petroleum ether (B4) – see Table 1 for experimental conditions. After each run the extracts samples were evaporated (in a rotary evaporator), weighed and analysed by GC-MS and FTIR-ATR.

2.4 Supercritical fluid extraction

A 0.5 L capacity Spe-ed^{TM} apparatus (Applied Sparations, USA) was used for the supercritical extraction experiments – the respective flowsheet is presented in Figure 2. In brief, liquid carbon dioxide is pressurized by a cooled liquid pump and mixed with cosolvent, followed by heating in a vessel until reaching the supercritical state. The biomass (*ca*. 50 g of cork per run) was previously placed in the extractor and then extracted with the supercritical solvent flowing upwards during 8h. The extract stream

is then depressurized, through a heated back pressure regulator valve (BPR), and bubbled in ethanol for subsequent yield quantification and chemical characterization. The spent CO_2 was vented to the atmosphere. Regarding the SFE assays with modifiers, the addition of cosolvent (ethanol) was accomplished using a liquid pump (LabAlliance Model 1500) coupled to the CO_2 line between the mass flow meter and the heating vessel. The SFE extracts were analyzed after ethanol evaporation. The SFE experimental conditions are presented in Table 1 (run SFE1 to SFE4).

2.5 Fourier Transform Infrared-Attenuated Total Reflectance (FTIR-ATR) spectroscopy analysis

A Bruker Tensor 27 spectrometer fitted with an attenuated total reflectance (ATR) accessory was used to collect FTIR spectra of Soxhlet, batch and SFE extracts. Pure friedelin and the original biomass were also analysed. The spectra was recorded in the wavelength region of 350-4000 cm^{-1} with 256 scans and a 4 cm^{-1} resolution. A baseline correction was also performed.

Table 1 – Experimental conditions for the extraction assays carried out.

Run	Type of extraction	Solvent	δ ($J^{1/2}$ $cm^{-3/2}$) [32]	$V_{solvent}$ (mL)	P (bar)	T (°C)	Q_{CO_2} (g min^{-1})	$m_{biomass}$ (g)	t (h)
S1	SLE-Soxhlet	MeOH	29.5	120	-	-	-	3.039	8
S2	SLE-Soxhlet	EtOH	26.4	120	-	-	-	3.018	8
S3	SLE-Soxhlet	DCM	20.4	120	-	-	-	3.055	8
S4	SLE-Soxhlet	PE	15.0	120	-	-	-	3.044	8
B1	SLE-Batch	MeOH	29.5	30	-	-	-	3.043	24
B2	SLE-Batch	EtOH	26.4	30	-	-	-	3.036	24
B3	SLE-Batch	DCM	20.4	30	-	-	-	3.041	24
B4	SLE-Batch	PE	15.0	30	-	-	-	3.050	24
SFE1	SFE	CO_2:EtOH (95.0:5.0 wt.%)	15.6	-	300	40	5	50.002	8
SFE2	SFE	CO_2:EtOH (97.5:2.5 wt.%)	14.7	-	300	40	8	50.002	8
SFE3	SFE	CO_2:EtOH (97.5:2.5 wt.%)	14.7	-	300	50	5	50.010	8
SFE4	SFE	CO_2:EtOH (97.5:2.5 wt.%)	14.7	-	300	60	8	50.035	8

EtOH – Ethanol; MeOH – Methanol; DCM – Dichloromethane; PE – Petroleum Ether; S – Soxhlet; SFE – Supercritical fluid extraction; SLE – Solid liquid extraction; δ - Hildebrand solubility parameter

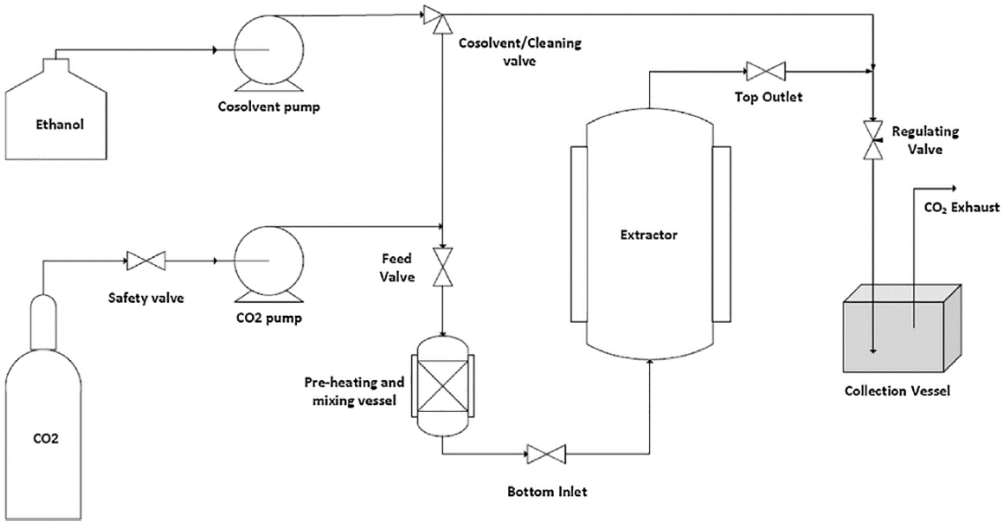

Figure 2 – Simplified flowsheet of the SFE unit of this work. Retrieved from [15]

2.6 Gas Chromatography Mass Spectroscopy (GC-MS) analysis

The GC-MS analysis procedure [33] is as follows: each dried sample (*ca.* 20 mg) was dissolved in 250 μL of pyridine containing 1 mg of tetracosane followed by the addition of 250 μL of BTSFA and 50 μL of TMSCl to promote the conversion of hydroxyl and carboxyl groups to trimethylsilyl (TMS) ethers and esters, respectively. This mixture was then maintained at 70 ℃ for 30 minutes [34]. For the quantitative analysis, tetracosane was used as internal standard (IS) and friedelin as external standard. Each extract was analyzed in duplicate and the reported results are the average of the measurements.

The GC-MS analyses were performed in a Shimadzu GCMS-QP2010 Ultra equipped with a DB-1 J&W capillary column (30 mm × 0.32 mm i.d., 0.25 μm film thickness and coupled with an auto-sampler. Helium was the carrier gas (40 $cm\,s^{-1}$) and the chromatographic conditions were as follows: initial temperature 80 ℃ for 5 min; heating rate 4 $℃\,min^{-1}$; final temperature 300 ℃ for 30 min; injector temperature 280 ℃; transfer-line temperature 290 ℃; split ratio 1:50. The MS was operated in the electron impact mode with electron impact energy of 70 eV and data collected at a rate of 0.1 scans s^{-1} over m/z range of 33-750. The ion source was maintained at 250 ℃.

2.7 Multidimensional scaling analysis

Multidimensional Scaling (MDS) was applied to the data collected from FTIR-ATR and GC-MS analysis. MDS is a method that represents the similarity (or dissimilarity) of multidimensional data as distances in a low-dimensional space in order to make these data accessible to visual analysis [35]. The MDS interpretation is based on the clusters and scalar distances between points in the plot obtained [36][37]. The method has been already applied in different areas such as physics [38], biology [39] and taxonomy [40]. In this work, the analysis was performed using IBM SPSS Statistics 23 software choosing Multidimensional Scalling (Proxscal), with the option "create proximities from data" with Euclidean distance as measure. The option to transform the results into values in the range from -1 to 1 was activated.

The application of MDS was based on two parameters. The first one corresponds to the similarity/dissimilarity between different samples which can be analysed graphically [36] and/or using a distance matrix [31]. The second parameter corresponds to the determination of the scaling stress value (*Stress*), which is a measure of the goodness of fit [41] associated to the scale reduction. In fact it measures the difference between the real multi-dimensional model and the reduced estimated space, and can be classified as: poor (if $Stress \leq 20$ %); fair (if $10\ \% \leq Stress < 20\ \%$); good (if $5\ \% \leq Stress < 10\ \%$); excellent (if $2.5\ \% \leq Stress < 5\ \%$) and perfect (if $Stress < 2.5\ \%$) [41][42].

The MDS modeling was applied to both FTIR-ATR spectra and GC-MS chromatograms. For the FTIR-AR spectra, the sixteen most relevant bands were selected and normalized in relation to methylene group stretching band, located at 2900 cm^{-1} [43]. This band was chosen since it is present in all spectra and cannot be used as a differentiation factor. As per the GC-MS, the sixteen most relevant peaks were selected, and their respective areas were normalized with the area of the internal standard considered in the analysis (tetracosane).

3. Results and discussion

3.1 Characterization of full extracts

3.1.1 Total extraction yield

The experimental results for total extraction yields (η_{Total}) are presented in Figure 3. A significant variability in η_{Total} values is evident, marked by the high yields obtained with polar solvents, namely methanol ($\delta = 29.5\ \mathrm{J}^{1/2}\ \mathrm{cm}^{-3/2}$) and ethanol ($\delta = 29.4\ \mathrm{J}^{1/2}\ \mathrm{cm}^{-3/2}$). The maximum value was attained for the Soxhlet extraction with methanol (η_{Total} = 13.8 wt.%) and the minimum was attained in batch solid-liquid extraction with petroleum ether (η_{Total} = 0.35 wt.%).

When compared with batch SLE and SFE, the Soxhlet yields were the largest. For batch SLE the η_{Total} values are comparable to SFE assays. These results show that the combination of fresh solvent in abundance with temperatures close to the solvent boiling point is a key advantage of Soxhlet extraction, which justify the general higher yields attainable through this method. Moreover, the robustness of the Soxhlet method can be evidenced by the η_{Total} attained (4.4 wt.%) using the solvent dichloromethane. This result is in agreement with the total yield of 4.02 wt.% reported by Şen *et al.* [19] for the same solvent. In turn, both Soxhlet and batch SLE extraction with petroleum ether (non-polar, $\delta = 14.988\ \mathrm{J}^{1/2}\ \mathrm{cm}^{-3/2}$) led to the lowest total yields, which highly contrasts with the maximum Soxhlet yield results for methanol and ethanol. These results emphasize the influence of the solvent power, particularly in what concerns the yield of lipophilic or hydrophilic extractives.

For SFE, the η_{Total} values ranged from 1.2 wt.% (run SFE3; 50 ℃, 2.5 wt.% EtOH, 5 $\mathrm{g\,min^{-1}}$) to 1.7 wt.% (run SFE4; 60 ℃, 2.5 wt.% EtOH, 8 $\mathrm{g\,min^{-1}}$). This maximum represents 38.6 % of the yield obtained by Soxhlet extraction with dichloromethane (DCM) and it is similar to the results obtained for batch SLE with the same solvent (i.e., η_{Total} = 1.4 wt.%). Furthermore, the maximum yield obtained for SFE represents only 50 % of the SFE practical and attainable total extraction yield ($X_0 =$ 3.4 wt. %, for SFE assays involving SC-CO_2 modified with 2.5 wt.% of ethanol) determined by Melo *et al.* [23] through phenomenological modelling for the same biomass. The positive impact of temperature and cosolvent (ethanol in this case) is also notorious: the highest values obtained correspond to the essay with higher ethanol content (run SFE1 with 5.0 wt.% EtOH) and to the essay with the highest temperature (run SFE4 with 60 ℃). Despite the better results of Soxhlet and batch SLE with

methanol, ethanol is the most used cosolvent in SFE because it is an innocuous solvent (both for human health and for the environment) in contrast with methanol [8].

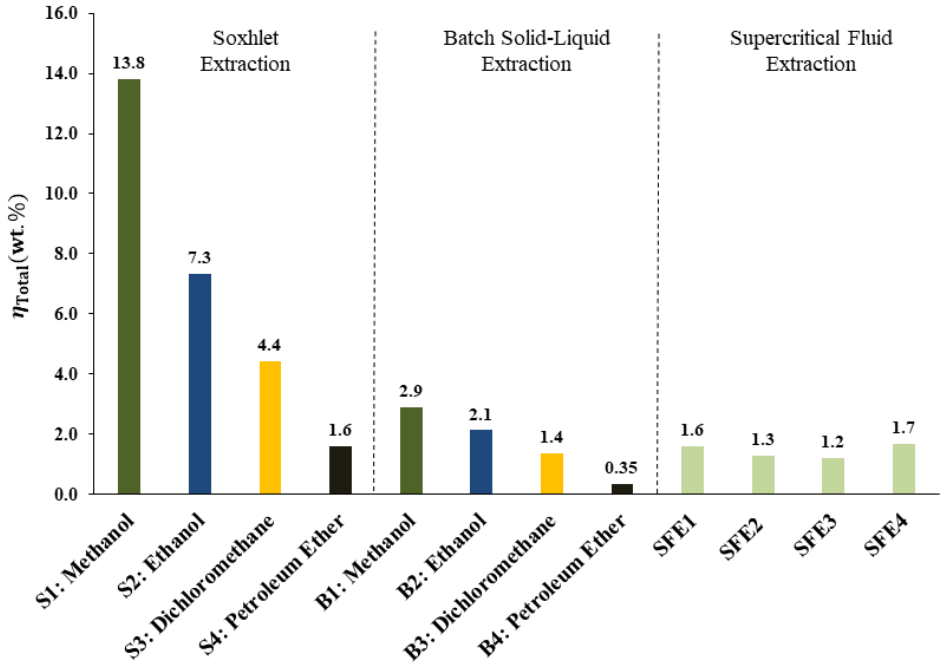

Figure 3 - Illustrative comparison of the total extraction yields from *Q. cerris* cork (20-40 mesh) obtained with different extractions methods and solvents. See Table 1 for experimental conditions.

3.1.2 Volatile extractives: friedelin yield and concentration

The bulk information provided by the total extraction yield results were complemented by GC-MS analyses to quantify the friedelin content in all extracts (see Figure 4 for a GC-MS chromatogram example). The results are presented in Table 2 in terms of friedelin extraction yield ($\eta_{\text{Friedelin}}$) and concentration of friedelin ($C_{\text{Friedelin}}$) in the extracts. Friedelin was the most abundant compound detected in agreement with previous studies [19][23]. The evaluation of its extraction is an important criteria to compare the attractiveness of the different solvents and extraction techniques.

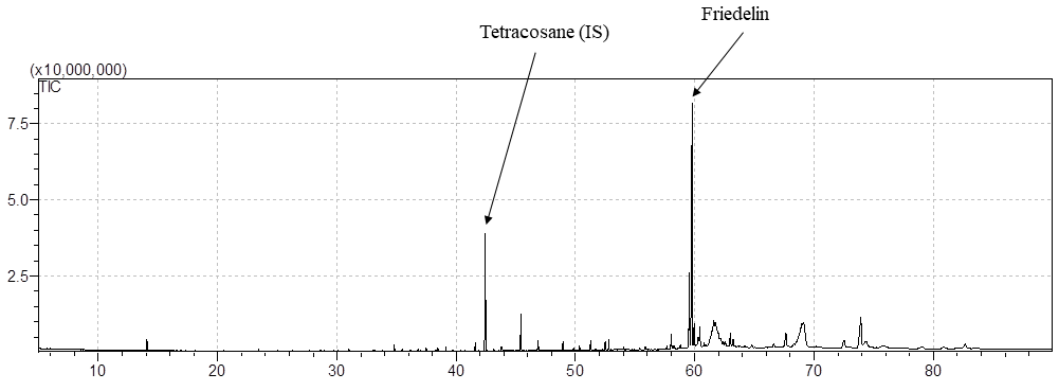

Figure 4 – GC-MS chromatogram of Soxhlet dichloromethane extract of Q. cerris cork. Tetracosane was used as internal standard (IS).

As per $\eta_{\text{Friedelin}}$, results ranged from 0.12 wt.% (run B4) to 1.68 wt.% (run S1). It can be observed that Soxhlet extractions (S1-S4) led to higher friedelin yields namely 1.68 wt.% with methanol, followed by 1.12 wt.% with ethanol and 1.05 wt.% with dichloromethane. These three solvents were the only ones who led to friedelin yields above 1 wt.% through Soxhlet. For batch SLE the highest yields were obtained with DCM (B3), that gave a $\eta_{\text{Friedelin}}$ value very similar to the results for all SFE assays. In fact, the friedelin yields obtained in SFE under different *T* and cosolvent conditions were rather similar, with the higher $\eta_{\text{Friedelin}}$ corresponding to SFE4 (60 ℃, 2.5 wt.% EtOH, 8 g min^{-1}). Moreover, friedelin extraction yields for SFE1 and SFE4 runs represent 54.0 % and 64.8 % (respectively) of the practical and attainable friedelin yield attainable by SFE ($X_0 =$ 0.74 wt. %), as reported by Melo *et al.* [23] for the same biomass.

Table 2 – Friedelin extraction yield and friedelin concentration of the Soxhlet, batch SLE and supercritical extractions.

Run	Type of extraction	Solvent	P (bar)	T (℃)	Q_{CO_2} (g min^{-1})	$\eta_{\text{Friedelin}}$ (wt.%)	$C_{\text{Friedelin}}$ (wt.%)
S1	SLE-Soxhlet	MeOH	-	-	-	1.68	12.1
S2	SLE-Soxhlet	EtOH	-	-	-	1.12	15.2
S3	SLE-Soxhlet	DCM	-	-	-	1.05	23.7
S4	SLE-Soxhlet	PE	-	-	-	0.67	41.3
B1	SLE-Batch	MeOH	-	-	-	0.16	5.4
B2	SLE-Batch	EtOH	-	-	-	0.14	6.4
B3	SLE-Batch	DCM	-	-	-	0.33	23.8
B4	SLE-Batch	PE	-	-	-	0.12	34.5
SFE 1	SFE	CO_2:EtOH (95:5 wt.%)	300	40	5	0.40	25.2
SFE 2	SFE	CO_2:EtOH (97.5:2.5 wt.%)	300	40	8	0.33	25.1
SFE 3	SFE	CO_2:EtOH (97.5:2.5 wt.%)	300	50	5	0.34	28.5
SFE 4	SFE	CO_2:EtOH (97.5:2.5 wt.%)	300	60	8	0.48	28.5

EtOH – Ethanol; MeOH – Methanol; PE – Petroleum Ether; DCM – Dichloromethane; S – Soxhlet; SFE – Supercritical fluid extraction; SLE – Solid liquid extraction.

In terms of friedelin concentration ($C_{\text{Friedelin}}$) the results (Table 2) exhibit pronounced differences ranging from 41.3 wt. % (run S4) to 5.4 wt. % (run B1). In contrast to the results obtained for η_{Total} (Figure 3), the best performing conditions were those involving weakly/non-polar solvents (petroleum ether, dichloromethane and SC-CO_2, where $\delta = 14.6 - 20.4$ $J^{1/2}$ $cm^{-3/2}$). This is certainly due to the great tendency of methanol and ethanol to also extract other polar extractives (such as phenolic compounds or sugars), which in turn dilute the fridelin content in those extracts. On the other hand, batch SLE reached $C_{\text{Friedelin}}$ values significantly lower than Soxhlet extractions with the same solvent which suggests that competitive solubilization of the extractives was unfavourable to friedelin. The only exception was DCM, which provided extracts with comparable friedelin content in both Soxhlet and batch SLE. In turn, these $C_{\text{Friedelin}}$ values are close to those reported by Şen *et al.*[19] ($C_{\text{Friedelin}} = 26.02\ \text{wt.}\%$). Remarkably, the SFE assays provided $C_{\text{Friedelin}}$ results that can be considered better than most Soxhlet and batch SLE, which once again confirms the interesting selectivity to friedelin previously demonstrated by the SFE technology [23].

3.1.3 FTIR-ATR results

Analysis by FTIR-ATR spectroscopy was applied to the Soxhlet extracts (S1 to S4), the batch SLE extracts (B1 to B4), the SFE extracts (SFE1 to SFE4), and also to the original *Q. cerris* cork (20-40 mesh) and pure friedelin. The resulting spectra can be observed in Figure 5, where the main bands were marked based on literature results [43][44]. In Figure 5, the spectra were sorted vertically to translate progressively simpler samples in terms of number of compounds: starting on the top with the original biomass (which can refer to the theoretical case of $\eta_{\text{Total}} = 100\ \text{wt.}\%$), and ending at the bottom with pure friedelin (theoretical case of $\eta_{\text{Total}} = \eta_{\text{Friedelin}}$).

A general overview of these spectra, the main bands identified correspond to: (i) carbohydrates and lignin related O-H vibration (e.g. O-H_{lignin}); (ii) the C-H stretching in methylene and methyl groups (CH_2 and CH_3); (iii) carbonyl stretching of suberin ester groups (C=O; C-O=C); (iv) aromatic ring vibration (C=C_{ar}) and deformation of C-H (C-H_{def}) of G-lignin; and (v) deformation of C-H of S-lignin (CH) and carbohydrates and lignin C-O vibration (C-O) [44][45]. In addition, bands at 1616 cm^{-1}, 1317 cm^{-1} and 500-800 cm^{-1} refer to the OH stretching of calcium oxalate monohydrate (whewellite) distributed in the phloem of *Q. cerris* bark [43][45]. Accordingly, since these calcium

oxalate acute bands were detected in the FTIR spectrum of our biomass, a non-neglibile presence of phloemic material (i.e. non cork) is present in the extracted samples, which corroborates previous results reported by Şen *et al.* [45]. On the other hand, looking at the bands associated to some polar groups present in biomass, namely O-H, C=O and C-O, their presence is notorious in methanol and ethanol extracts (S1 , S2, B1 and B2), but they lose importance in spectra for the other solvent extracts, becoming negligible (e.g. supercritical extracts SFE1-SFE4). This fact highligths the affinity of methanol and ethanol to remove compounds with strong polar bonds when compared to dichloromethane, petroleum ether and also supercritical CO_2. In fact, since the SFE1-SFE4 assays comprise CO_2 modified with ethanol, the respective FTIR-ATR spectra suggest that the used amounts of cosolvent (2.5-5.0 wt.%) are not able to increment the solubilization of sugars or phenolic compounds (O-H). Similar results regarding cosolvent effects were reported by Rodrigues et al. [15] for *Eucalyptus globulus* leaves extraction. Last but not least, the peaks associated to pure friedelin FTIR spectra (with emphasis to the carbonyl carbon C=O, see Figure 1a) have particulary acute shape for extracts obtained with weakly/non-polar solvents. This suggests the predominance of this molecule in those extracts, thus corroborating the higher aforementioned values of $C_{\text{Friedelin}}$.

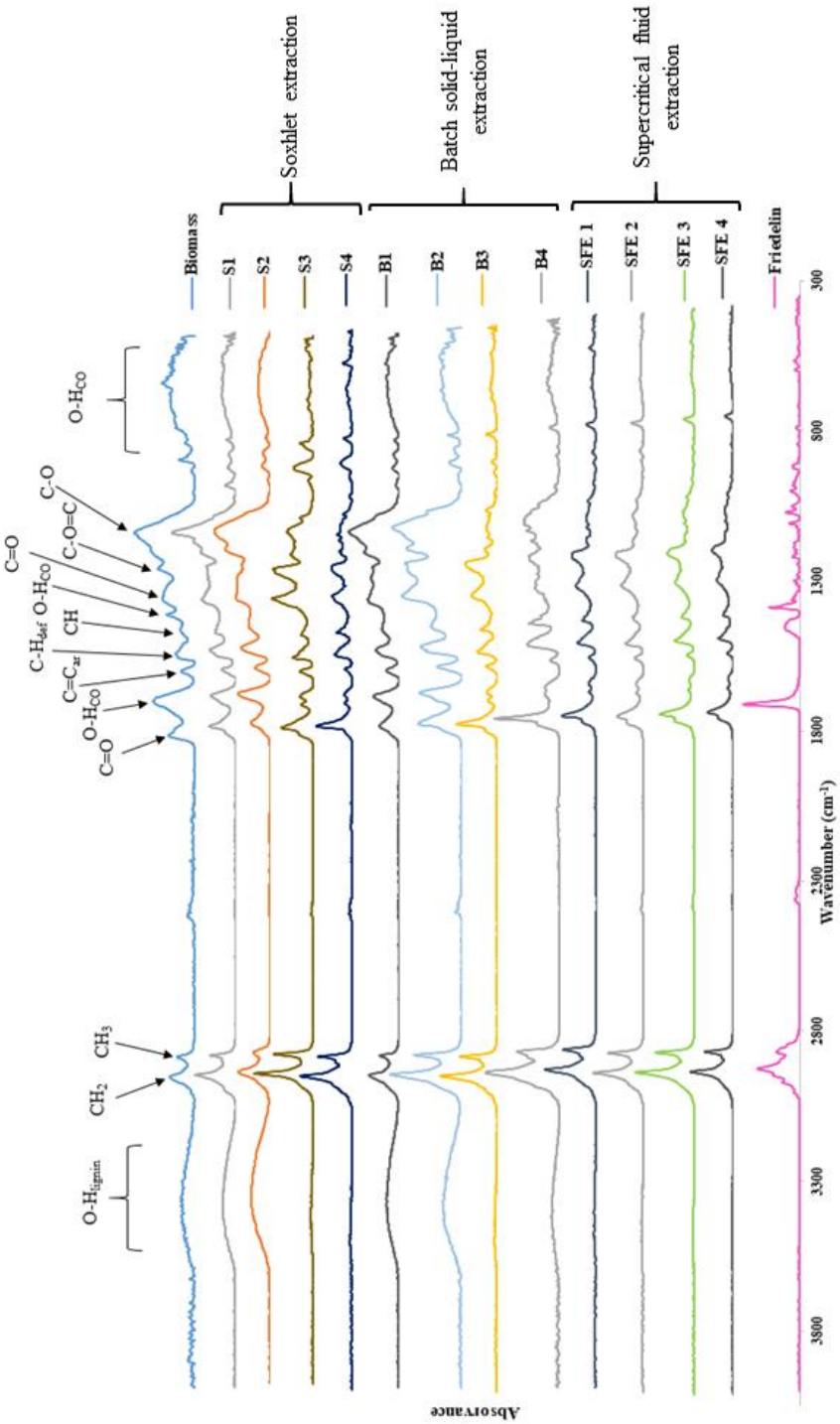

Figure 5 – FTIR-ATR spectra of Soxhlet, batch SLE and supercritical extracts, of original biomass sample and pure friedelin

3.2 Multidimensional scaling analysis

As referred in Section 2, MDS was applied to FTIR-ATR spectra and GC-MS chromatograms of the different extracts produced. This multivariate statistic method has advantages over other methods since it can unveil similarity/dissimilarity relations based on several distinct metrics [37]. Accordingly, Table 3 compiles the full list of 16 spectrum peaks and 16 chromatogram peaks considered for the analysis, which represents the starting point for the targeted scale reduction. In both cases, these were selected using a criteria of quantitative relevance (magnitudes).

Table 3 - Compilation of the selected FTIR-ATR spectra peaks (in wavenumber units) and the associated chemical and GC-MS peaks (in retention time units) with the corresponding compound for the MDS analysis.

Dimension	FTIR-ATR peak	Associated bond	GC-MS peaks	Compound
#1	721 cm^{-1}	O-H	14.1 min	Glycerol
#2	781 cm^{-1}	O-H	34.8 min	Hexadecanoic acid
#3	816 cm^{-1}	O-H	38.5 min	11-Octadecanoic acid
#4	877 cm^{-1}	O-H	45.4 min	Docosanoic acid
#5	1032 cm^{-1}	C-O	48.9 min	Squalene
#6	1157 cm^{-1}	C-O=C	52.8 min	n.i.
#7	1261 cm^{-1}	C=O	58.0 min	β-Sitosterol
#8	1317 cm^{-1}	O-H	59.5 min	Triterpene n.i.
#9	1469 cm^{-1}	CH	59.8 min	Friedelin
#10	1452 cm^{-1}	C-H	59.9 min	Triterpene n.i.
#11	1514 cm^{-1}	$C=C_{ar}$	60.4 min	Triterpene n.i.
#12	1616 cm^{-1}	O-H	60.7 min	Triterpene n.i.
#13	1736 cm^{-1}	C=O	63.0 min	Betulin
#14	1909 cm^{-1}	C=O	67.6 min	Triterpene n.i.
#15	2850 cm^{-1}	CH_3	72.5 min	Triterpene n.i.
#16	3355 cm^{-1}	O-H	73.9 min	Triterpene n.i.

C_{ar} – Aromatic carbon; n.i. – not identified; Triterpene n.i. – triterpene not identified

Stress values for the three different cases studied (i.e. GC-MS, FTIR-ATR, and their combination) are presented in Table 4 for a preliminary analysis of the method regarding the intended scale reduction. Regarding scale reduction to 2D, the stress values point to goodness of fit classifications between good (10.4 % and 7.6 %) and excellent (4.7 %) in the case of GC-MS. In contrast, the further reduction to 1D downgrades goodness of fit to poor (26.3 % and 21.5%) and good (8.6 %). In general, these results demonstrate the effort to simplify the information of 16 dimensions (GC-MS chromatograms data, and FTIR-ATR spectra) or 32 dimensions (combination GC-MS and FTIR-ATR) is feasible for 2 dimensions. Moreover, the jump from 2D to 1D is itself a specific source of a non-negligible decrease of the goodness of fit, particularly when FTIR-ATR data is involved. Nevertheless, since higher stress values do not imply necessarily a loss of the scientific value of the analysis [35], the 1D representation of data was preferred, as it allows an easier interpretation of the results, namely the visualization of the similarities/dissimilarities of the chemical composition of the extracts produced by different methods and solvents.

Table 4 – Stress values for the scale reduction of FTIR-ATR and GC-MS multidimensional data.

	Stress (%)	
	1 Dimension (1D)	2 Dimension (2D)
FTIR-ATR	26.3	10.4
GC-MS	8.6	4.7
FTIR-ATR + GC-MS	21.5	7.6

The MDS map (1D) for FTIR-ATR data is represented in Figure 6a, and includes not only the extracts results, but also the respective 16 spectrum peaks of the original biomass and of the pure friedelin spectra. A logical result is the highest distance observed between the cork matrix and the pure friedelin. Then, a diminution of the extracts complexity from left to right is notorious, with Soxhlet and batch SLE extracts produced with polar solvents (S1, S2, B1, B2) positioned closer to the biomass. This is certainly due to higher total extraction yields attained by these solvents and to the fact that the enrichment of the extracts with polar extractives turn their composition (chemical bonds) more representative of the original biomass. Moving to the right, an intermediate zone stands out grouping together all the SFE extracts (SFE1 to SFE4), plus B3 and S4, which are the petroleum ether batch SLE and the DCM Soxhlet. These score very short distances between each other, and are slightly apart from S3 and B4,

which exhibit an offset to left, towards an increased proximity to the extracts obtained with polar solvents. While the subtle distinction between S3/B4 and B3/S4 was not expected, it can be explained by the greater difficulty of FTIR-ATR data analysis to ensure the intended dimensional reduction to 1D (denoted by the higher *Stress* value). On the other hand, from the perspective of the approximation to pure friedelin, the MDS results are in agreement with the $C_{\text{Friedelin}}$ values reported in Section 3.1.2 for most of the extracts (see e.g. S4, SFE3 and SFE4 results in Table 2), excepting once again B4 sample. Lastly, the FTIR-ATR results reinforce the proximity between the chemical composition of Soxhlet extracts using DCM and SFE, even if 5 wt.% modified SC-CO_2 is used.

Moving to the GC-MS MDS map (1D) represented in Figure 6b, friedelin was maintained in the analysis as it could be analysed by GC-MS (its retention time is 59.8 min). However the same does not apply to the cork biomass since it cannot be directly analysed by GC-MS. Regarding the results obtained, a different horizontal display of friedelin was attained (on the left side), but such position difference is irrelevant for the interpretation of the results, as only the absolute distances have a meaning in the MDS method. Globally, the scale reduction of the extracts volatiles suggest a grouping in two distinct clusters. The first one comprises the alcoholic extracts (S1, S2, B1 and B2), and stands farther from the pure friedelin. This once again suggests that the higher total extraction yield obtained with these solvents is due to the extraction of other compounds besides friedelin. The second cluster refers to the extracts from the weakly and non-polar solvents, regardless of the extraction method. In fact, the pronounced proximity between SFE, and dichloromethane and petroleum ether extracts point to a strong similarity between the volatile compounds extracted with these solvents, which agrees with the results presented for friedelin concentration in Section 3.1.2. Moreover, the slight modification of SC-CO_2 with ethanol does not seem to impose strong deviations on the composition of the extracts, and thus corroborates the moderate tuning of polarity accomplished by the addition of this cosolvent [8]. A final remark on this map is the apparent better behaviour of MDS in the reduction to 1D, which can be ascribed to the absence of cork biomass in the analysis, but also to the fact that GC-MS data cover only information from a fraction of the full extract composition, comprising thus a simplification of the chemical complexity prone to be found in extracts from vegetal species.

Finally, in figure 6c MDS results are presented for a combination of GC-MS and FTIR-ATR data aiming an even richer (but more demanding) comparison between extracts. Accordingly, two main extracts clusters were found once again: one encompassing alcoholic extracts and the other including the extracts from weakly and non-polar solvents. The main difference corresponds to the major balance between these clusters in relation to pure friedelin. Here, one must recall that while GC-MS results refer to individual compounds abundances, FTIR-ATR is related to the general chemical bonds prevailing in the group of molecules found in an extract. In fact, the combination of spectroscopic and chromatographic data seems to demonstrate a clear correlation between the chemical nature of the cork extracts with the polarity of the extraction solvent, and how much closer the extracts from nonpolar solvents (including modified SC-CO_2) are, in general, from the target compound friedelin.

On the whole, the effort to interpret multidimensional chemical data with the MDS method opened the way to an insightful demonstration that, more than the extraction method (Soxhlet, Batch, or SFE), what imposes major differences in the chemical composition of the produced extracts is the intrinsic polarity of the solvent. As a result, the reported results emphasize in great extent the need for a trade-off between total extraction yields and the yields/concentrations of target compounds, as distinct solvents (and extraction methods) can be deemed preferable for each of these goals.

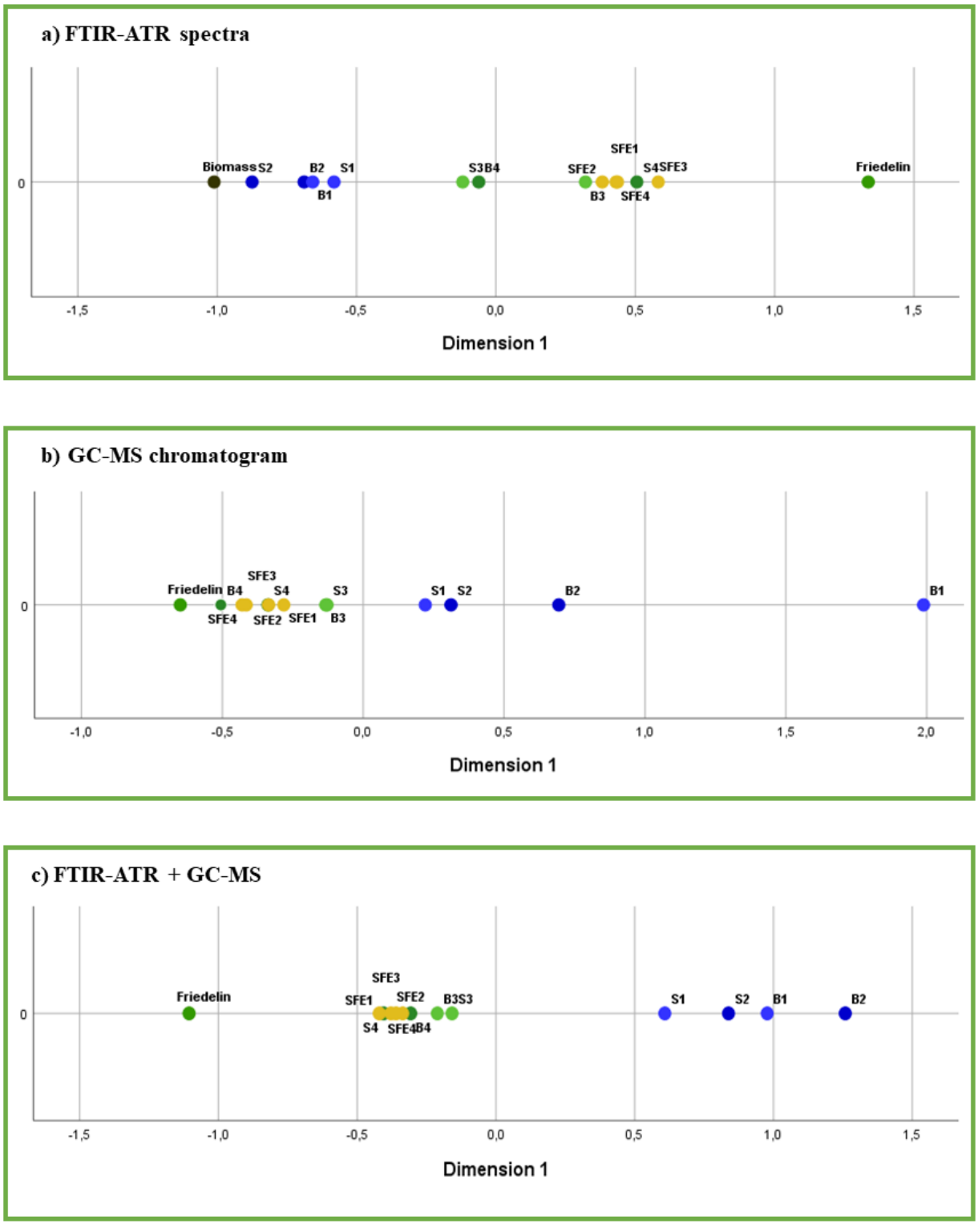

Figure 6 – MDS maps of: (a) FTIR-ATR, (b) GC-MS and (c) both FTIR-ATRT and GC-MS.

4. Conclusions

The present study comprises a comparison and characterization study on the experimental extraction of *Quercus cerris* cork with methanol, ethanol, dichloromethane, petroleum ether using both Soxhlet and batch solid-liquid extraction (SLE), and with modified carbon dioxide through supercritical fluid extraction (SFE). The maximum total extraction yield (η_{Total}) was attained for the Soxhlet extraction with methanol (η_{Total} = 13.8 wt.%) and the minimum was attained in batch SLE with petroleum ether (η_{Total} = 0.35 wt.%). A significant variability of η_{Total} values was evident, marked by the higher yields obtained with polar solvents, namely methanol and ethanol. In turn, the η_{Total} values obtained for batch SLE are comparable to those of SFE assays. For the supercritical fluid extractions, η_{Total} ranged from 1.2 wt.% for run SFE3 (50 ℃, 2.5 wt.% EtOH, 5 g min^{-1}) to 1.7 wt.% for run SFE4 (60 ℃, 2.5 wt.% EtOH, 8 g min^{-1}). In addition, the positive impact of temperature and cosolvent in SFE was also notorious, being the highest values obtained for the essay with higher ethanol content or with the highest temperature.

In terms of friedelin extraction yields ($\eta_{\mathrm{Friedelin}}$), results ranged from 0.12 wt.% (batch SLE with petroleum ether) to 1.68 wt.% (Soxhlet with methanol). Soxhlet extractions with alcoholic solvents led to higher friedelin yields. Batch SLE with dichloromethane and all SFE assays presented similar $\eta_{\mathrm{Friedelin}}$ results. As for friedelin concentration ($C_{\mathrm{Friedelin}}$), the results ranged from 41.3 wt. % (Soxhlet with dichloromethane) to 5.4 wt. % (batch SLE with methanol). In fact, the best performing assays on $C_{\mathrm{Friedelin}}$ were those involving weakly/non-polar solvents. Batch extractions reached $C_{\mathrm{Friedelin}}$ values significantly lower than Soxhlet extractions with the same solvent which suggests that competitive solubilisation of the extractives was unfavourable to friedelin. The SFE assays provided $C_{\mathrm{Friedelin}}$ results better than most Soxhlet and batch SLE experiments, which confirms the interesting selectivity to friedelin enabled by this extraction method.

MDS analysis of FTIR-ATR and GC-MS was advantageously used to unveil that more than the extraction method (Soxhlet, Batch, or SFE) it is the intrinsic polarity of the solvent what makes major impact in the chemical composition of the produced extracts. In general, the alcoholic extracts were more distinct from the pure friedelin and closer to biomass, and contrast with extracts from the weakly and non-polar solvents, which scored invariably closer to pure friedelin. The results match with the fact that

FTIR-ATR spectra of the extracts highligth the affinity of methanol and ethanol to remove compounds with strong polar bonds when compared to dichloromethane, petroleum ether and also supercritical CO_2. In contrast, the chemical bonds associated to pure friedelin (particularly the carbonyl carbon C=O) have particulary acute signals in extracts produced with weakly/non-polar solvents.

On the whole, the reported study emphasized how the most aggressive operating conditions do not always lead to the best results, particularly those that depend on specific chemical trade-offs and not on intensity. In fact, the optimum conditions depend on what is the main goal of extraction: an extract enriched in a higher diversity of compounds (higher total extraction yield), or in a target compound like friedelin.

5. References

[1] F. Chemat, M. A. Vian, and G. Cravotto, "Green Extraction of Natural Products: Concept and Principles," *Int. J. Mol. Sci.*, vol. 13, no. 7, pp. 8615–8627, Jul. 2012.

[2] C. M. G. C. Renard, "Extraction of bioactives from fruit and vegetables: State of the art and perspectives," *LWT*, vol. 93, pp. 390–395, Jul. 2018.

[3] M. D. Luque de Castro and F. Priego-Capote, "Soxhlet extraction: Past and present panacea," *J. Chromatogr. A*, vol. 1217, no. 16, pp. 2383–2389, 2010.

[4] C. H. Chan, R. Yusoff, and G. C. Ngoh, "Modeling and kinetics study of conventional and assisted batch solvent extraction," *Chem. Eng. Res. Des.*, vol. 92, no. 6, pp. 1169–1186, 2014.

[5] F. Amarni and H. Kadi, "Kinetics study of microwave-assisted solvent extraction of oil from olive cake using hexane: Comparison with the conventional extraction," *Innov. Food Sci. Emerg. Technol.*, vol. 11, no. 2, pp. 322–327, Apr. 2010.

[6] Z. Pan, W. Qu, H. Ma, G. G. Atungulu, and T. H. McHugh, "Continuous and pulsed ultrasound-assisted extractions of antioxidants from pomegranate peel,"

Ultrason. Sonochem., vol. 19, no. 2, pp. 365–372, Mar. 2012.

[7] N. Boussetta, E. Vorobiev, V. Deloison, F. Pochez, A. Falcimaigne-Cordin, and J.-L. Lanoisellé, "Valorisation of grape pomace by the extraction of phenolic antioxidants: Application of high voltage electrical discharges," *Food Chem.*, vol. 128, no. 2, pp. 364–370, Sep. 2011.

[8] M. M. R. De Melo, A. J. D. Silvestre, and C. M. Silva, "Supercritical fluid extraction of vegetable matrices: Applications, trends and future perspectives of a convincing green technology," *J. Supercrit. Fluids*, vol. 92, pp. 115–176, 2014.

[9] H. Passos, M. G. Freire, and J. A. P. Coutinho, "Ionic liquid solutions as extractive solvents for value-added compounds from biomass," *Green Chem.*, vol. 16, no. 12, pp. 4786–4815, Nov. 2014.

[10] C. B. Mehr, R. N. Biswal, J. L. Collins, and H. D. Cochran, "Supercritical carbon dioxide extraction of caffeine from guaraná," *J. Supercrit. Fluids*, vol. 9, no. 3, pp. 185–191, Sep. 1996.

[11] A. F. M. Cláudio, A. M. Ferreira, M. G. Freire, and J. A. P. Coutinho, "Enhanced extraction of caffeine from guaraná seeds using aqueous solutions of ionic liquids," *Green Chem.*, vol. 15, no. 7, p. 2002, Jun. 2013.

[12] A. M. da Costa Lopes, M. Brenner, P. Falé, L. B. Roseiro, and R. Bogel-Łukasik, "Extraction and Purification of Phenolic Compounds from Lignocellulosic Biomass Assisted by Ionic Liquid, Polymeric Resins, and Supercritical CO2," *ACS Sustain. Chem. Eng.*, vol. 4, no. 6, pp. 3357–3367, Jun. 2016.

[13] M. Cvjetko Bubalo, S. Vidović, I. Radojčić Redovniković, and S. Jokić, "New perspective in extraction of plant biologically active compounds by green solvents," *Food Bioprod. Process.*, vol. 109, pp. 52–73, May 2018.

[14] T. Inoue, S. Tsubaki, K. Ogawa, K. Onishi, and J. Azuma, "Isolation of

hesperidin from peels of thinned Citrus unshiu fruits by microwave-assisted extraction," *Food Chem.*, vol. 123, no. 2, pp. 542–547, Nov. 2010.

[15] V. H. Rodrigues, M. M. R. de Melo, I. Portugal, and C. M. Silva, "Extraction of *Eucalyptus* leaves using solvents of distinct polarity. Cluster analysis and extracts characterization," *J. Supercrit. Fluids*, vol. 135, no. January, pp. 263–274, 2018.

[16] C. P. Passos, R. M. Silva, F. A. Da Silva, M. A. Coimbra, and C. M. Silva, "Supercritical fluid extraction of grape seed (*Vitis vinifera L.*) oil. Effect of the operating conditions upon oil composition and antioxidant capacity," *Chem. Eng. J.*, vol. 160, no. 2, pp. 634–640, Jun. 2010.

[17] S. P. Silva, M. A. Sabino, E. M. Fernandes, V. M. Correlo, L. F. Boesel, and R. L. Reis, "Cork: properties, capabilities and applications," *Int. Mater. Rev.*, 2005.

[18] A. Şen, T. Quilho, and H. Pereira, "Bark anatomy of *Quercus cerris L. var. cerris* from Turkey," *Turk. J. Botany*, vol. 35, pp. 45–55, 2011.

[19] A. Şen, M. M. R. De Melo, A. J. D. Silvestre, H. Pereira, and C. M. Silva, "Prospective pathway for a green and enhanced friedelin production through supercritical fluid extraction of *Quercus cerris* cork," *J. Supercrit. Fluids*, vol. 97, pp. 247–255, 2015.

[20] A. Şen, I. Miranda, and H. Pereira, "Temperature-induced structural and chemical changes in cork from *Quercus cerris*," *Ind. Crops Prod.*, vol. 37, no. 1, pp. 508–513, 2012.

[21] A. Şen, T. Quilhó, and H. Pereira, "The cellular structure of cork from *Quercus cerris var. cerris* bark in a materials' perspective," *Ind. Crops Prod.*, vol. 34, no. 1, pp. 929–936, 2011.

[22] A. Şen, I. Miranda, S. Santos, J. Graça, and H. Pereira, "The chemical composition of cork and phloem in the rhytidome of *Quercus cerris* bark," *Ind.*

Crops Prod., vol. 31, no. 2, pp. 417–422, 2010.

[23] M. M. R. de Melo, A. Şen, A. J. D. Silvestre, H. Pereira, and C. M. Silva, "Experimental and modeling study of supercritical CO2 extraction of *Quercus cerris* cork: Influence of ethanol and particle size on extraction kinetics and selectivity to friedelin," *Sep. Purif. Technol.*, vol. 187, pp. 34–45, 2017.

[24] B. Lu, L. Liu, X. Zhen, X. Wu, and Y. Zhang, "Anti-tumor activity of triterpenoid-rich extract from bamboo shavings (*Caulis bamfusae* in Taeniam)," vol. 9, no. 38, pp. 6430–6436, 2010.

[25] P. Antonisamy, V. Duraipandiyan, and S. Ignacimuthu, "Anti-inflammatory, analgesic and antipyretic effects of friedelin isolated from *Azima tetracantha Lam.* in mouse and rat models," *J. Pharm. Pharmacol.*, vol. 63, no. 8, pp. 1070–1077, 2011.

[26] A. Ricci, K. J. Olejar, G. P. Parpinello, P. A. Kilmartin, and A. Versari, "Application of Fourier Transform Infrared (FTIR) Spectroscopy in the Characterization of Tannins," *Appl. Spectrosc. Rev.*, vol. 50, no. 5, pp. 407–442, May 2015.

[27] A. Leghissa, Z. L. Hildenbrand, and K. A. Schug, "A review of methods for the chemical characterization of cannabis natural products," *J. Sep. Sci.*, vol. 41, no. 1, pp. 398–415, Jan. 2018.

[28] Y. Q. Li, D. X. Kong, and H. Wu, "Analysis and evaluation of essential oil components of cinnamon barks using GC-MS and FTIR spectroscopy," *Ind. Crops Prod.*, vol. 41, no. 1, pp. 269–278, 2013.

[29] M. De Luca *et al.*, "Derivative FTIR spectroscopy for cluster analysis and classification of morocco olive oils," *Food Chem.*, vol. 124, no. 3, pp. 1113–1118, 2011.

[30] P. R. A. B. de Toledo, M. M. R. de Melo, H. R. Pezza, A. T. Toci, L. Pezza, and C. M. Silva, “Discriminant analysis for unveiling the origin of roasted coffee samples: A tool for quality control of coffee related products,” *Food Control*, vol. 73, pp. 164–174, Mar. 2017.

[31] A. Difusa, K. Mohanty, and V. V. Goud, “The chemometric approach applied to FTIR spectral data for the analysis of lipid content in microalgae cultivated in different nitrogen sources,” *Biomass Convers. Biorefinery*, vol. 6, no. 4, pp. 427–433, 2016.

[32] C. L. Yaws, *Chemical Properties Handbook*. 1999.

[33] M. M. R. de Melo, E. L. G. Oliveira, A. J. D. Silvestre, and C. M. Silva, “Supercritical fluid extraction of triterpenic acids from *Eucalyptus globulus* bark,” *J. Supercrit. Fluids*, vol. 70, pp. 137–145, Oct. 2012.

[34] R. M. A. Domingues, M. M. R. De Melo, E. L. G. Oliveira, C. P. Neto, A. J. D. Silvestre, and C. M. Silva, “Optimization of the supercritical fluid extraction of triterpenic acids from *Eucalyptus globulus* bark using experimental design,” *J. Supercrit. Fluids*, vol. 74, pp. 105–114, 2013.

[35] I. Borg and P. J. F. Groenen, *Modern multidimensional scaling: theory and applications*. Springer, 1997.

[36] A. M. Lopes and J. A. Tenreiro Machado, “Analysis of temperature time-series: Embedding dynamics into the MDS method,” *Commun. Nonlinear Sci. Numer. Simul.*, vol. 19, no. 4, pp. 851–871, Apr. 2014.

[37] A. M. Lopes, J. P. Andrade, and J. A. Tenreiro Machado, “Multidimensional scaling analysis of virus diseases,” *Comput. Methods Programs Biomed.*, vol. 131, pp. 97–110, 2016.

[38] K. Hollemeyer, W. Altmeyer, E. Heinzle, and C. Pitra, “Matrix-assisted laser

desorption/ionization time-of-flight mass spectrometry combined with multidimensional scaling, binary hierarchical cluster tree and selected diagnostic masses improves species identification of Neolithic keratin sequences from furs o," *Rapid Commun. Mass Spectrom.*, vol. 26, no. 16, pp. 1735–1745, Aug. 2012.

[39] C. Tzagarakis, T. A. Jerde, S. M. Lewis, K. Uğurbil, and A. P. Georgopoulos, "Cerebral cortical mechanisms of copying geometrical shapes: a multidimensional scaling analysis of fMRI patterns of activation," *Exp. Brain Res.*, vol. 194, no. 3, pp. 369–380, Apr. 2009.

[40] D. A. Lacher and P. F. Lehmann, "Application of multidimensional scaling in numerical taxonomy: Analysis of isoenzyme types of Candida species," *Ann. Clin. Lab. Sci.*, vol. 21, no. 2, pp. 94–103, 1991.

[41] H. Dumanoglu *et al.*, "Analyses of fruit attributes by multidimensional scaling method of apple genetic resources from coastal zone of North Eastern Anatolia, Turkey," *Sci. Hortic. (Amsterdam).*, vol. 240, no. February, pp. 147–154, 2018.

[42] J. B. Kruskal, "Multidimensional scaling by optimizing goodness of fit to a nonmetric hypothesis," *Psychometrika*, vol. 29, no. 1, pp. 1–27, 1964.

[43] A. Şen, A. V. Marques, J. Gominho, and H. Pereira, "Study of thermochemical treatments of cork in the 150-400°C range using colour analysis and FTIR spectroscopy," *Ind. Crops Prod.*, vol. 38, no. 1, pp. 132–138, 2012.

[44] M. H. Lopes, C. Pascoal Neto, A. S. Barros, D. Rutledge, I. Delgadillo, and A. M. Gil, "Quantitation of aliphatic suberin in *Quercus suber L.* Cork by FTIR spectroscopy and solid-state13C-NMR spectroscopy," *Biopolym. - Biospectroscopy Sect.*, vol. 57, no. 6, pp. 344–351, 2000.

[45] A. Şen, T. Quilhó, and H. Pereira, "Bark anatomy of *Quercus cerris L. var. cerris* from Turkey," *Turk J Bot*, vol. 35, pp. 45–55, 2011.

III. Publication 2

Optimization of the supercritical fluid extraction of *Quercus cerris* cork: influence of operating conditions on total extraction yield, friedelin concentration and selectivity.

Pedro G. Vieira[1], Marcelo M.R. de Melo[1], Ali Şen[2], Mário M.Q. Simões[3], Inês Portugal[1], Helena Pereira[2], Carlos M. Silva[1]*

[1] CICECO – Aveiro Institute of Materials, Department of Chemistry, University of Aveiro, Aveiro 3810-193, Portugal

[2] Centro de Estudos Florestais, Instituto Superior de Agronomia, Universidade de Lisboa, Tapada da Ajuda, 1349-017 Lisboa, Portugal

[3] QOPNA, Department of Chemistry, University of Aveiro, Aveiro, Portugal

Keywords:

Supercritical fluid extraction, Friedelin, *Quercus cerris*, Cork, Design of experiments, Response surface method, Selectivity

1. Introduction

Cork is a very important material in the industry due to its unique properties namely the compressibility, impermeability and low thermal conductivity. The cork oak tree (*Quercus suber*) is the most known species, and is used for the production of stoppers for the wine industry [1], [2]. Many other products are obtained from cork such as insulation and surfacing materials [2], and some studies report its use as effective sorbent for the removal of heavy metals in waste water [3], [4].

The industrial transformation of cork produces large amounts of residues. For example, during cork stoppers production, cork powder represents 30 % of the raw material [5]. In the case of the bark of Turkey oak (*Quercus cerris*), it is only used as fuel for energy production [6]. However, the extraction of chemicals from these residues has raised interest due to their possible bioactive applications.

In recent years, the extractives of *Q. cerris* have been studied with different extraction processes and solvents. One of the most important extractives is friedelin ($C_{30}H_{50}O$), a pentacyclic triterpene ketone, which besides anti-oxidant activity [7] exhibits valuable bioactive properties such as analgesic [8], antipyretic [8], anti-inflammatory [8], anti-tumor [9], and it is useful for slowing the progress of some oxidative stress-related diseases [7]. Moreover, Corticeira Amorim (a Portuguese cork company) has already patented [10] a solid-liquid extraction method followed by purification of friedelin present in cork and cork-derived materials, which demonstrates the high economic potential of this compound.

Recent studies [6, 11] report that *Q. cerris* cork can render a total extraction yield (η_{Total}) of 11 wt.% for Soxhlet extraction with dichoromethane, Supercritical fluid extraction (SFE) is a green extraction technique that has been successfully applied to the extraction of vegetable matrices [12], including *Q. cerris* cork. Accordingly, Şen *et al.* [6] have shown that friedelin can be obtained from *Q. cerris* using supercritical CO_2 (at 300 bar and 40-60 ℃) in concentrations between 30.4-40.6 wt.%. Moreover, Melo *et al.* [11] focused the impact of the particle size and cosolvent (ethanol) concentration on total extraction yield (η_{Total}) and friedelin extraction yield ($\eta_{\mathrm{Friedelin}}$). These authors presented important arguments on how particle size, ethanol content and carbon dioxide flow rate affect the production of friedelin-enriched extracts. In the case of particle size, intermediate granulometries (from 20-40 mesh to 60-80 mesh) were shown to be advantageous instead of smaller particles (> 80 mesh) or coarse particles. Also, a clear

improvement of selectivity towards friedelin was demonstrated for higher extraction times. Moreover, it was also stated that the use of ethanol as cosolvent can significantly enhance the total extraction yield. However, intermediate contents of this cosolvent are preferable (*ca.* 2.5 wt.%) in terms of selectivity to friedelin, otherwise an abundant removal of non-target extractives prevails [11].

At this point, it is pertinent to study the influence of the SFE operating conditions upon the extraction of *Q. cerris* cork, namely the cosolvent content, CO_2 flow rate and extraction temperature. For this study, a Design of Experiments (DoE) combined with the Response Surface Methodology (RSM) is applied in order to map and model the individual and crossed influence of these parameters towards the identification of optimum operation regions of enhanced production of friedelin-enriched extracts. This methodology has been successfully applied within the topic of SFE of natural matrices, for example spent coffee grounds [13], hemp (*Cannabis sativa* L.) seeds [14], *Eucalyptus globulus* bark [15], Persimmon (*Diospyros kaki L.*) [16] and some others [12].

The structure of the present document is the following one: Section 2 (Materials and Methods) is devoted to the presentation of the biomass and chemicals used (Section 2.1), the supercritical extraction process (Section 2.2) and the design of experimental and statistical modeling (Section 2.2). Section 3 covers the Results and Discussion and comprises to following subsections: Experimental optimization of the SFE operating conditions (Section 3.1), which is divided into the analysis of the total extraction yield, friedelin concentration and selectivity to friedelin (Sections 3.1.1, 3.1.2 and 3.1.3, respectively). It is followed by the experiments at optimal operating conditions (Section 3.2), and by validation testes carried out on the fitted models (Section 3.3). Finally Section 4 presents the main conclusions of the work.

2. Materials and methods

2.1 Chemicals and biomass samples

Ethanol (purity 99.5 %) and dichloromethane (purity, 99.98 %) were supplied by Fisher Scientific (Leicestershire, United Kingdom). Pyridine (purity 99.5 %), N,O-Bis(trimethylsilyl)trifluoroacetamine (BTSFA, purity 98 %), chlorotrimethylsilane (TMSCl, purity 99 %) and friedelin (95 % purity) were supplied by Sigma Aldrich (Deutschland). CO2 (purity 99 %) was supplied by Air Liquide (Algés, Portugal).

Q. cerris bark was obtained from Kahramanmaras, Turkey, and was granulated with a hammer-type industrial mill. The resulting granules were separated by density difference in distilled water, with 10 minutes mixing time. The floating fraction of cork-enriched granules (subsequently named cork) was dried and grinded into 20-40 mesh (0.42-0.84 mm), which can be considered a trade-off particle size between the minimization of the industrial effort associated to milling and the expectable yield and selectivity performances, according to a previous study [11]. The moisture content of the biomass was experimentally measured by drying *ca.* 3 g of cork at 60 ℃ for 24h. The sample was weighed before and after drying, being the moisture 5.6 wt.%.

2.2 Extraction processes

Soxhlet extraction was carried out during 8 h, using *ca.* 3 g of 20-40 mesh *Q. cerris* cork and 120 mL of dichloromethane as solvent. The batch solid-liquid extraction was accomplished in a sealed beaker for 24 h, periodically shaking (manually) the vessel. Accordingly, cork (*ca.* 3 g) was extracted individually with dichloromethane (30 mL) in a 1:10 w/v ratio. By the end of both processes, the extract samples were evaporated, weighed and analyzed by GC-MS.

Supercritical extractions experiments were performed in a 0.5 L capacity Speed^{TM} apparatus (Applied Separations, USA), whose flowsheet can be seen in Figure 1. Initially, the liquid carbon dioxide is pressurized by a cooled liquid pump, and then mixed with cosolvent (ethanol). The next step comprises heating the liquid stream in a vessel to reach the supercritical state before entering the extractor. The supercritical solvent flows upwards through the extractor where the biomass was previously loaded (*ca.* 45 g of cork per run). The extract stream is then depressurized through a heated back pressure regulator valve (BPR) and bubbled in ethanol for subsequent yield quantification and chemical characterization. Therefore, the solutes remain trapped in a cooled chamber containing the collection vessel partially filled with ethanol, while the

spent CO_2 is vented to the atmosphere. Regarding the SFE assays with modifiers, the addition of cosolvent (ethanol) was accomplished using a liquid pump (LabAlliance Model 1500) coupled to the CO_2 line between the mass flow meter and the heating vessel. Lastly, the extracts were analyzed after ethanol evaporation.

In this work, total extraction yield (η_{Total}), friedelin concentration in the extracts ($C_{\text{Friedelin}}$), and the selectivity to friedelin ($\alpha_{\text{F,nF}}$) were investigated as process outputs. Their determination was performed according to the following expressions:

$$\eta_{\text{Total}}(\text{wt.}\,\%) = \frac{w_{\text{extract}}}{w_{\text{biomass}}} \times 100 \tag{1}$$

$$\eta_{\text{Friedelin}}(\text{wt.}\,\%) = \frac{w_{\text{Friedelin}}}{w_{\text{biomass}}} \times 100 \tag{2}$$

$$\eta_{\text{non-Friedelin}}\,(\text{wt.}\,\%) = \eta_{\text{Total}} - \eta_{\text{Friedelin}} \tag{3}$$

$$C_{\text{Friedelin}}(\text{wt.}\,\%) = \frac{w_{\text{Friedelin}}}{w_{\text{extract}}} \times 100 \tag{4}$$

$$\alpha_{\text{F,nF}} = \frac{\eta_{\text{Friedelin}} \times \left[X_{0,\text{non-Friedelin}} - \eta_{\text{non-Friedelin}}\right]}{\eta_{\text{non-Friedelin}} \times \left[X_{0,\text{Friedelin}} - \eta_{\text{Friedelin}}\right]} \tag{5}$$

where w_{extract} is the mass of dry extract, $w_{\text{biomass}}$is the mass of cork used in the experiment, and $w_{\text{Friedelin}}$ is the mass of extracted friedelin and quantified by GC-MS. $X_{0,\text{Friedelin}}$ and $X_{0,\text{non-Friedelin}}$ are the friedelin and non-friedelin concentrations in the raw material, which were determined in a previous modeling study [11].

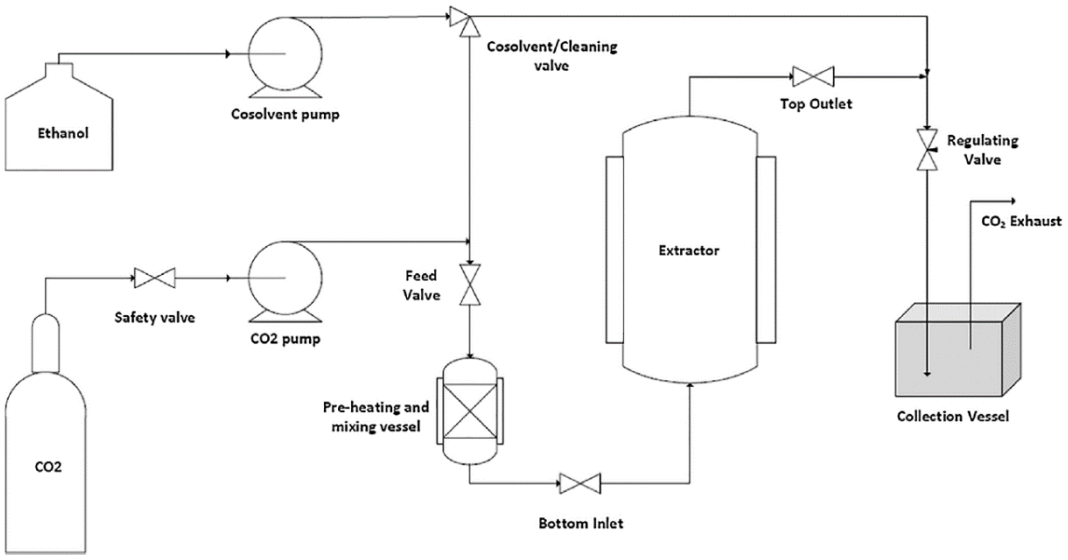

Figure 1 - Simplified flowsheet of the SFE unit of this work. Retrieved from [17].

2.3 Design of Experiments and Response Surface Methodology (DoE/RSM)

Response surface methodology (RSM) is an useful technique for developing, improving and optimizing processes in which a response (dependent variable) is influenced by several factors (independent variables) [18]. The main objective is to optimize this response, and quantify and describe the impact of each studied factor and their combined interactions. In addition, this experimental methodology also fits empirical models relating these factors and their interactions with the experimental responses. In turn, design of experiments (DoE) allows more precise and complete information to be obtained while minimizing the number of assays and material costs needed.

In this work, the influence of the operating conditions was studied using a Box-Behnken design (BBd) of three factors and three levels, totalizing 15 experiments. The chosen factors and respective levels were the extraction temperature (*T*), measured at 40-50-60 ℃; ethanol concentration (EtOH wt.%), at 0.0-2.5-5.0 wt.%; and CO_2 flow rate (Q_{CO_2}), at 5-8-11 g min^{-1}. The remaining operating conditions were fixed along the experiments namely, pressure ($P = 300$ bar), extraction time ($t = 8$ h), and particle size, ($d_p = 20 - 400$ mesh). The lab assays were randomized in order to minimize unknown and uncontrollable effects on the results (nuisance factor).

The independent variables are listed in Table 1 and were codified as follows:

$$X_k = \frac{x_k - x_0}{\Delta x_k} \quad (6)$$

where X_k is the codified value of the independent variable x_k, x_0 is its real value at the central point, and Δx_k is the step change between levels for the k variable.

Table 1 - Correspondence of the different levels and factors considered in codified and non-codified format.

Variable		Level correspondence		
		Low (-1)	Medium (0)	High (+1)
x_1: Temperature (ºC)	*T*	40	50	60
x_2: EtOH contente (wt.%)	EtOH	0.0	2.5	5.0
x_3: CO_2 flow rate (g min^{-1})	Q_{CO_2}	5	8	11

Experimental SFE results analyzed by RSM are usually well described by a second order polynomial function such as:

$$Y = \beta_0 + \sum_{i=1}^{3} \beta_i X_i + \sum_{i=1}^{3} \beta_{ii} X_i^2 + \sum_{i=1}^{3} \sum_{j=i+1}^{3} \beta_{ij} X_i X_j \quad (7)$$

where Y is the studied response (whether η_{Total}, $C_{\mathrm{Friedelin}}$ or $\alpha_{\mathrm{F,nF}}$), β_0 is a constant, β_i are model coefficients associated to linear effects, β_{ii} are coefficients linked to quadratic effects, and β_{ij} are coefficients for interaction effects.

STATISTICA software (version 5.1, StatSoft Inc., Tulsa, USA) was used in this work. An analysis of variance (ANOVA) was employed to assess the statistically significant factors and interactions using Fisher's test and its associated probability p(F). In addition, t-tests were applied to judge the significance of the estimated coefficients of each model. Determination coefficients, R^2, and adjusted determination coefficients, R^2_{adj}, were used to evaluate the goodness of the fit of the regression model [19], as follows:

$$R^2 = 1 - \frac{SS_E}{SS_T} \quad (8)$$

$$R^2_{\mathrm{adj}} = 1 - \frac{\frac{SS_E}{(n-p)}}{\frac{SS_T}{(n-1)}} \quad (9)$$

where SS_E represents the error sum of squares, SS_T represents the total sum of squares, *n* and *p* represent the total number of assays and the degrees of freedom, respectively.

2.4Gas Chromatography Mass Spectroscopy (GC-MS) analysis

Before each GC-MS analysis, *ca.* 20 mg of dried extract was converted into trimethylsilyl (TMS) derivates according to the literature [20]. The applied procedure is as follows: each dried sample was firstly dissolved in 250 µL of pyridine containing 1 mg of tetracosane. The addition of 250 µL of BTSFA and 50 µL of TMSCl promotes the conversion of compounds with hydroxyl and carboxyl groups to TMS ethers and esters, respectively. This mixture was then maintained at 70 °C for 30 minutes [15]. Each extract was analyzed in duplicate with tetracosane as internal standard. The reported results are the average of these measurements.

The GC-MS analyses were performed in a Shimadzu GCMS-QP2010 Ultra equipped with a DB-1 J&W capillary column (30 mm × 0.32 mm i.d., 0.25 µm film

thickness) and coupled with an auto-sampler. Helium was the carrier gas (40 $cm\ s^{-1}$) and the chromatographic conditions were as follows [6]: initial temperature of 80 ℃ for 5 min; heating rate at 4 ℃ min^{-1}; final temperature of 300 ℃ for 30 min; injector temperature of 280 ℃; transfer-line temperature of 290 ℃; split ratio of 1:50. The MS was operated in the electron impact mode with electron impact energy of 70 eV and data collected at a rate of 0.1 scans s^{-1} over a range of m/z of 33-750. The ion source was maintained at 250 ℃.

3. Results and discussion

3.1 Experimental optimization of the SFE operating conditions

The results of the fifteen SFE runs are presented in Table 2, along with the corresponding experimental conditions. The total extraction yields ranged from 0.6 wt.% in run SFE5 [50 ℃, 0.0 wt.% EtOH, 5 g min^{-1}] to 2.2 wt.% in runs SFE11 [50 ℃, 5.0 wt.% EtOH, 11 g min^{-1}] and SFE15 [60 ℃, 5.0 wt.% EtOH, 8 g min^{-1}]. Despite being half of the yield obtained by Soxhlet extraction with dichloromethane (4.3 wt.%, Table 2), the highest SFE yield is 46.6 % times greater than that of batch solid-liquid extraction (SLE) with the same solvent (1.5 wt.%, Table 2). Nonetheless it is worth noting that, in the case of Soxhlet extraction, the separation is favored by the use of fresh solvent at boiling temperature. Moreover, the SFE maximum yield represents only 64.7% of the SFE practical attainable total extraction yield ($X_0 =$ 3.4 wt. %, for SFE assays involving SC-CO_2 modification with 5 wt.% of ethanol), as reported by Melo *et al.* [11].

Considering the friedelin concentration in the supercritical extracts, its values ranged from 25.3 wt.% in run SFE7 [50 ℃, 2.5 wt.% EtOH, 8 g min^{-1}] to 36.2 wt. % in run SFE2 [40 ℃, 2.5 wt.% EtOH, 5 g min^{-1}], which means they are all superior than those of the Soxhlet extracts ($C_{\mathrm{Friedelin}}$ = 24.2 wt.%) and solid-liquid extracts ($C_{\mathrm{Friedelin}}$ = 24.0 wt.%). It is also particularly notorious that similar values of $C_{\mathrm{Friedelin}}$ can be achieved under distinct operating conditions, i.e. combining different temperatures, flow rates and ethanol contents (see Table 2).

Finally, the selectivity towards friedelin ranged from 1.1 in run SFE7 [50 ℃, 2.5 wt.% EtOH, 8 g min^{-1}] to 3.1 in run SFE11 [50 ℃, 5 wt.% EtOH, 11 g min^{-1}]. It is important to emphasize that all $\alpha_{\mathrm{F,nF}}$ values are higher than 1.0 and that the maximum attained is higher than the selectivities reported by Melo *et al.* [11] for the same particle size of *Q. cerris* cork but for an extraction time of 6 h.

Table 2 – Experimental conditions and results of the extraction assays carried out in this work. Pressure, particle size and extraction time were held constant at 300 bar, 20-40 mesh and 8 h, respectively.

Run	T (°C)	EtOH content (wt.%)	Q_{CO_2} (g min^{-1})	η_{Total} (wt. %)	$C_{Friedelin}$ (wt. %)	$\alpha_{F,nF}$
SFE1	40	0.0	8	1.0	34.2	2.0
SFE2	40	2.5	5	1.0	36.2	2.3
SFE3	40	2.5	11	1.3	31.3	1.8
SFE4	40	5.0	8	1.5	29.3	1.6
SFE5	50	0.0	5	0.6	33.2	1.7
SFE6	50	0.0	11	1.1	29.0	1.4
SFE7	50	2.5	8	1.3	25.3	1.1
SFE8	50	2.5	8	1.4	26.5	1.3
SFE9	50	2.5	8	1.1	29.0	1.5
SFE10	50	5.0	5	1.6	30.5	1.9
SFE11	50	5.0	11	2.2	33.0	3.1
SFE12	60	0.0	8	1.3	32.1	1.8
SFE13	60	2.5	5	1.0	28.4	1.4
SFE14	60	2.5	11	1.6	29.7	1.7
SFE15	60	5.0	8	2.2	32.0	2.7
Soxhlet extraction with dichloromethane				4.3	24.2	-
Solid-liquid extraction with dichloromethane				1.5	24.0	-

To jointly compare the impacts of the studied factors (including their interactions) on the results, Pareto charts of the effects are represented in Figure 2, one for each response. The black and white colors indicate the type of influence (numerically positive or negative, respectively) of each factor/interaction. Effects whose bars are shorter than the statistical significance line (vertical line) can be considered non-significant for a confidence level of 95 %, in the case of η_{Total}, or 90 % in the case of $C_{Friedelin}$ and $\alpha_{F,nF}$. The two latter responses were initially tested for a 95 % confidence level but none of the effect bars positioned above the statistical significance threshold. This occurrence results from the more balanced distribution of the effects magnitude upon these responses (see Figures 2b and 2c), which hinders the existence of isolated influential factors or interactions for a stricter confidence level (case of Figure 2a), as further discussed below.

In terms of η_{Total} (Figure 2a), the three individual factors (EtOH, Q_{CO_2} and T) stand as the most significant, all with a linear positive impact on η_{Total}. Among these, the linear effect of EtOH content is by far the most influent operating condition, causing stronger enhancements of η_{Total}. This behavior emphasizes the important role played by cosolvent due to the modification of polarity imparted to the SC-CO_2. In turn, the second most influent factor was Q_{CO_2}, being *ca*. 42.6 % lower than EtOH. In any case, an increase of the CO_2 flow rate (from 5 to 11 g min^{-1}) is able to improve η_{Total} values,

as in generally shown in Table 2. This is certainly due to the film resistance to mass transfer that may prevail at lower flow rate and reduce the extraction rate. Additionally, for the lower Q_{CO_2} assays, the accumulation of solutes in the fluid phase inside the extractor may also occur and decrease the driving force to mass transfer. In the case of T, its effect bar lies in the vicinity of the statistically significance exclusion limit, with p = 0.053. From a thermodynamic point of view, an increment of temperature gives rise to two opposing effects in supercritical fluids: while it reduces the solvent power through density reduction, on the other hand it enhances solubility by increasing the vapor pressure of the solutes (friedelin and others) [6]. Remarkably, within the range of our experimental conditions, a positive impact of temperature was observed, which means that vapor pressure growth prevails over density reduction. For example, under fixed CO_2 flow rate and ethanol content, an increase from 40 to 60 ℃ (SFE4 and SFE15) represented an enhancement of 46.7 % in the value of η_{Total}. This result clearly detaches from studies reported for other species [13], [15], where lower temperatures led to higher η_{Total} values.

For the $C_{\mathrm{Friedelin}}$ response (Figure 2b), the quadratic impact of ethanol content (EtOH× EtOH) and of temperature ($T \times T$) both scored the most significant and positive effects. An important result in this graph is the non-observance of the Pareto principle in the sorting of the effects (i.e., 20/80 rule), being observed instead a step like arrangement of the bars, whose individual magnitudes do not exceed 2.5 units (contrarily to the Pareto of η_{Total} effects in Figure 2a). This justifies the need to consider a 90 % confidence level to ensure statistical significance of some effects. The positive sign of all quadratic effects suggests that non-linear jumps might be expected, and that a region of minimum friedelin concentration may be expected. Furthermore, the combined effect of CO_2 flow rate with ethanol or temperature ($\mathrm{EtOH} \times Q_{CO_2}$ or $T \times Q_{CO_2}$) contributes also with a positive synergy to $C_{\mathrm{Friedelin}}$ values.

For the selectivity towards friedelin ($\alpha_{\mathrm{F,nF}}$), the respective Pareto chart allows a direct insight on the great influence of ethanol on $\alpha_{\mathrm{F,nF}}$, as all effects involving cosolvent content were ranked on top and with numerical positive importance. In fact, a common feature of the three Pareto charts is the prevalence of positive effects in relation to negative ones. On the other hand, experimental data seem to be in agreement with this behavior (see Table 2).

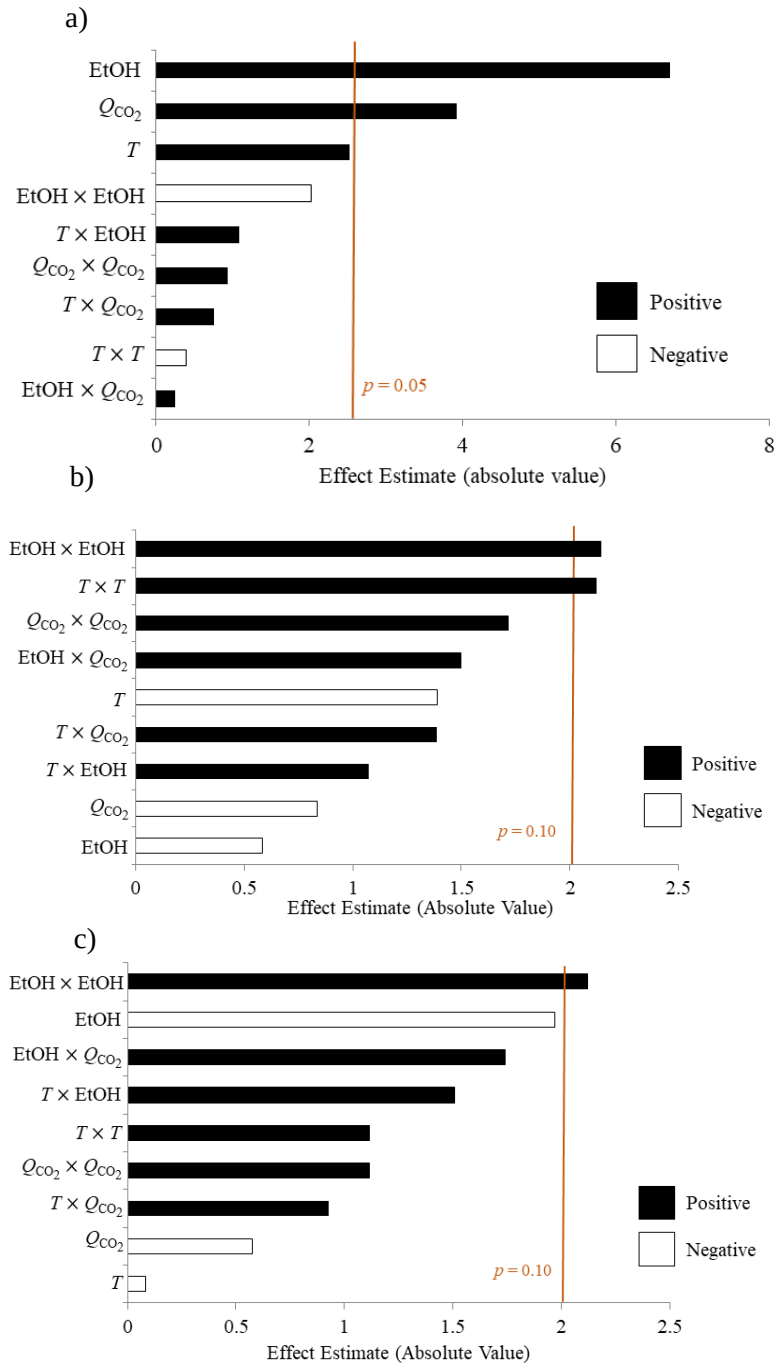

Figure 2 – Pareto charts for the supercritical fluid extraction of *Q. cerris* cork, showing the influence of factors on the (a) total extraction yield (η_{Total}), (b) friedelin concentration in the extract ($C_{\mathrm{Friedelin}}$), and (c) selectivity towards friedelin ($\alpha_{\mathrm{F,nF}}$).

In what concerns the regression modeling of η_{Total} , $C_{\mathrm{Friedelin}}$ and $\alpha_{\mathrm{F,nF}}$, data from Table 2 were coded according to Eq. (6) and submitted to RSM analysis in order to determine the individual and crossed coefficients of Eq. (7). These coefficients obtained are listed in Table 3, where the statistically significant coefficients at 95% (for η_{Total}) or 90 % (for $C_{\mathrm{Friedelin}}$ and $\alpha_{\mathrm{F,nF}}$) confidence levels are marked in bold. For total extraction yield, the attained results are in accordance with the information given by the Pareto diagram in Figure 2a: only four parameters can be considered statistically significant, namely β_0, β_1, β_2 and β_3, which correspond to the typical constant of the polynomial model and the linear effects of temperature, ethanol content and the CO_2 flow rate, respectively.

For $C_{\mathrm{Friedelin}}$ and $\alpha_{\mathrm{F,nF}}$, the results are also in agreement with the information already evidenced by the Pareto charts in Figures 2b and 2c, respectively. Nevertheless, to ensure a reasonable goodness of fit for optimization purposes, the non-significant contributions of $Q_{\mathrm{CO_2}} \times Q_{\mathrm{CO_2}}$, $\mathrm{EtOH} \times Q_{\mathrm{CO_2}}$, T and $T \times Q_{\mathrm{CO_2}}$ (all having effect estimates above 1.4 units, see Figure 2b) were maintained for the fitting of the $C_{\mathrm{Friedelin}}$ surface model, and an analogous strategy was adopted for $\alpha_{\mathrm{F,nF}}$. This approach gives rise to the moderate gap between the values of R^2 and the R^2_{adj} shown in Table 3 for the full models, particularly in the case of $C_{\mathrm{Friedelin}}$ and $\alpha_{\mathrm{F,nF}}$. The reduced models (RM) were refitted to the data and then converted to uncoded variables by substitution of Eq. (6) in the respective terms of Eq. (7). The final expressions for each response are shown in Table 4.

Table 3 – Regression coefficients of the RSM polynomial given by Eq. (7), their individual significance at 90 %/95% confidence level and respective determination coefficients for the full model (FM); values in bold represents significant coefficients.

	η_{Total}		$C_{\mathrm{Friedelin}}$		$\alpha_{\mathrm{F,nF}}$	
	FM	*p*	FM	*p*	FM	*p*
β_0	1.31921	**<0.001**	144.25509	**<0.001**	14.62361	**0.003**
β_1	-0.05008	**0.053**	-3.11417	0.223	-0.33708	0.938
β_2	-0.20483	**0.001**	-6.36833	0.584	-1.31000	**0.106**
β_3	0.12051	**0.011**	-6.91065	0.440	-0.87361	0.590
β_{11}	0.00038	0.710	0.02471	**0.087**	0.00250	0.315
β_{22}	0.03127	0.098	0.39933	**0.085**	0.07600	**0.088**
β_{33}	-0.0100	0.395	0.22180	0.147	0.02780	0.315
β_{12}	0.0040	0.329	0.0480	0.332	0.01300	0.192
β_{13}	0.0023	0.483	0.0517	0.224	0.00670	0.396
β_{23}	0.0030	0.817	0.2233	0.194	0.05000	0.142
R^2	0.937		0.789		0.768	
R^2_{adj}	0.823		0.410		0.351	

Table 4 – Reduced experimental models (RM) fitted to the responses listed in Table 2.

Response	Reduced model	R^2	R^2_{adj}	Eq.
η_{Total} (wt.%)	$\eta_{Total} = -0.6038 + 0.0165\,T + 0.1755\,\mathrm{EtOH} + 0.085417\,Q_{CO_2}$	0.845	0.803	(10)
$C_{Friedelin}$ (wt.%)	$C_{Friedelin} = 136.026 - 2.994\,T + 0.0247\,T^2 - 3.783\,\mathrm{EtOH} + 0.399\,\mathrm{EtOH}^2 - 6.690\,Q_{CO_2} + 0.222 Q_{CO_2}{}^2 + 0.0517\,T \times Q_{CO_2} + 0.223\mathrm{EtOH} \times Q_{CO_2}$	0.697	0.470	(11)
$\alpha_{F,nF}$	$\alpha_{F,nF} = 12.128 - 0.282\,T + 0.0025\,T^2 - 1.310\,\mathrm{EtOH} + 0.076\,\mathrm{EtOH}^2 - 0.569\,Q_{CO_2} + 0.028 Q_{CO_2}{}^2 + 0.013\,T \times Q_{CO_2} + 0.05\mathrm{EtOH} \times Q_{CO_2}$	0.713	0.497	(12)

3.1.1 Total extraction yield

The two fitted response surfaces for η_{Total} (Eq. (10)) are shown in Figure 3. Figure 3a shows that an increase of the CO_2 flow rate has a slightly stronger impact on η_{Total} when compared with temperature, and thus when both factors are simultaneously increased to their maximum, a positive synergy is obtained and the highest total extraction yield is attained. In turn, Figure 3b (with temperature fixed at 50 ℃) shows a surface with a greater slope (comparing with Figure 3a), which stresses the major impact of cosolvent content and of CO_2 flow rate on the η_{Total} response. For the lowest values of these two operating conditions (i.e., 0 wt.% and 5 g min^{-1}), the model predicts the smallest total extraction yield, in agreement with experimental data. Furthermore, with the highest quantity of ethanol (i.e., 5.0 wt.%) one can obtain greater yields than when the CO_2 flow rate is at its maximum, which confirms the individual effects impact graphed in Figure 2a.

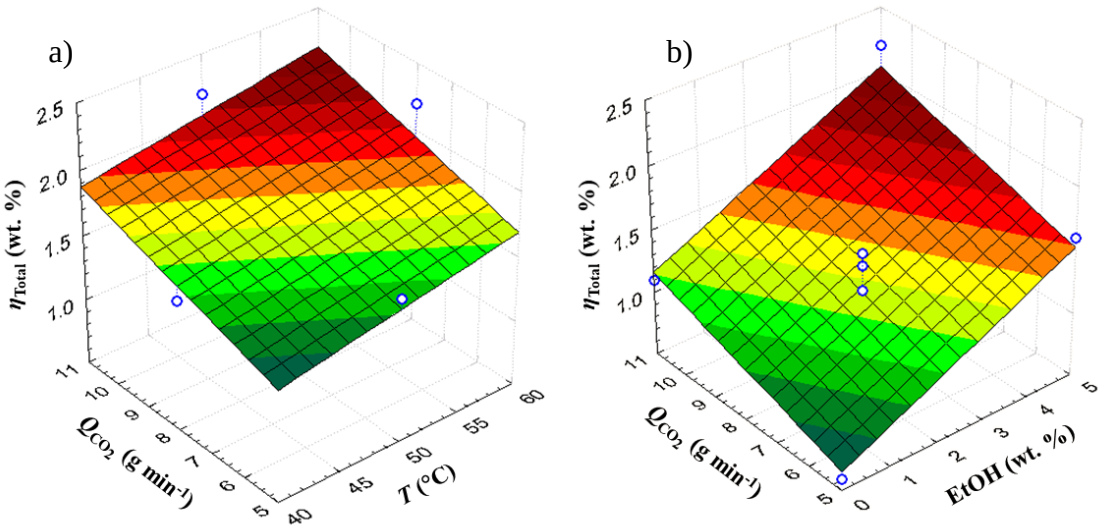

Figure 3 – Response surfaces plotting the effects of (a) temperature and carbon dioxide flow rate on total extraction yield, for 5 wt.% EtOH content, and (b) ethanol content and carbon dioxide flow rate on total extraction yield, at 50 ℃ . Dots are experimental data and response surfaces are given by Eq. (10).

3.1.2 Friedelin concentration

The fitted $C_{\text{Friedelin}}$ surface response is plotted in Figure 4, along with the experimental results. It can be observed that the visual aspect of these plots is rather different from those of η_{Total} model (Figure 3) notwithstanding being represented by the same independent variables and conditions. Furthermore, the fitting quality can be checked visually, with some data points lying farther from the predicted values (R^2=0.697).

In Figure 4a, the higher temperatures and lower CO_2 flow rates (under constant 5 wt.% EtOH) lead to a region of lower friedelin contents, amounting ca. 29 wt.%. In contrast, the highest friedelin content results are predicted for the combination of higher flow rates and temperatures, which agrees with the positive synergy of the combination of these factors depicted in the Pareto chart (Figure 2b). Furthermore, Figure 4b displays the positive effect of the combination of ethanol content and CO_2 flow rate. Accordingly, for a temperature of 50 ℃, the model predicts the higher friedelin concentration in two situations: (i) when ethanol content and flow rate are both increased, or (ii) for lower values of these two factors simultaneously.

According to the reduced model, the operating conditions that provide the maximization of friedelin concentration in *Q. cerris* extracts ($C_{\text{Friedelin}}$= 38.2 wt.%) are the combination of a lower temperature (40 ℃) without cosolvent addition (0 wt.% EtOH) and lower CO_2 flow rate (5 g min^{-1}). This is a remarkable example on how the most aggressive conditions don't always lead to the best results, particularly those that depend on specific chemical trade-offs and not so much on the separation power.

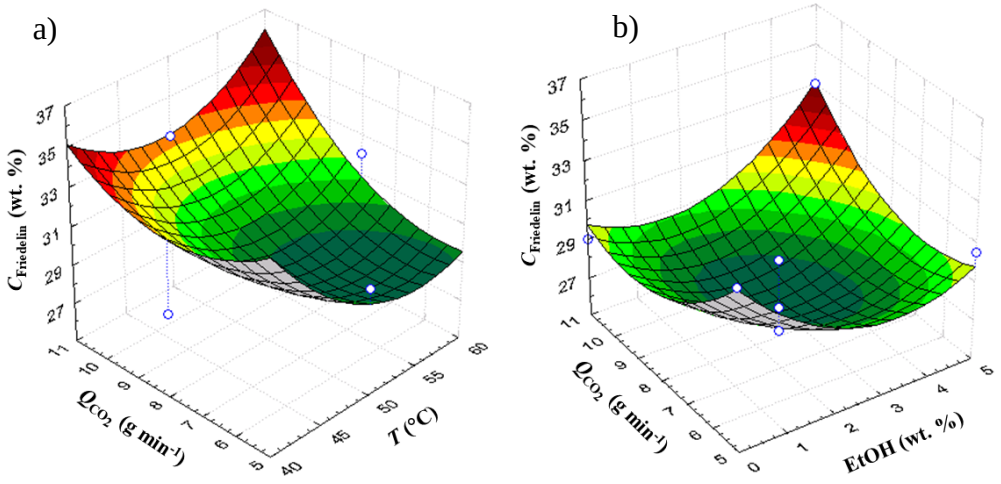

Figure 4 - Response surface plotting the effects of (a) temperature and carbon dioxide flow rate on friedelin concentration for 5 wt.% EtOH content and (b) ethanol content and carbon dioxide flow rate on friedelin concentration at 50℃ (reduced model). Dots are experimental data and surface response is given by Eq. (11)

3.1.3 Selectivity to friedelin

In the case of $\alpha_{F,nF}$, the plotted surface is presented in Figure 5 for an ethanol content of 5 wt.% (Figure 5a), and for a temperature of 50 ℃ (Figure 5b). The goodness of fit (R^2=0.713) similar to those obtained for $C_{Friedelin}$ can be visually checked upon the analysis of the surfaces and experimental data (points). Within the experimental space considered the model predicts selectivity values higher than 1.0, which means that one can expect friedelin to be removed selectively within any combination of the studied operating conditions. Moreover, in Figure 5a the positive effect of the combination of CO_2 flow rate and temperature can be visualized, which is in agreement with the insights from the respective Pareto chart (Figure 2c). Accordingly, an increase of both factors at the same time leads to a remarkably high selectivity of 3.1 (predicted value using Eq. 12).

Moreover, Figure 5b shows the real impact of ethanol on $\alpha_{F,nF}$. Accordingly, for a constant flow rate of 11 g min^{-1}, an ethanol content jump from 0 to 5 wt.% results in an enhancement of selectivity of ca. 92.8 %, increasing from 1.4, to 2.7. In turn, the same cosolvent variation at lower flow rates induces more moderate (but still advantageous) gains of $\alpha_{F,nF}$. In fact, the positive effect of ethanol (as cosolvent) in selectivity was also reported by Melo et al. [11] for extraction time of 6 h, but their study pointed to 2.5 wt.% as the most favorable content. In turn, our is $\alpha_{F,nF}$ = 3.3 (at *t* = 8.0 h), and that it can be obtained at the highest levels of each factor, i.e. 60 ℃, 5 wt.% EtOH, and 11 g min^{-1}.

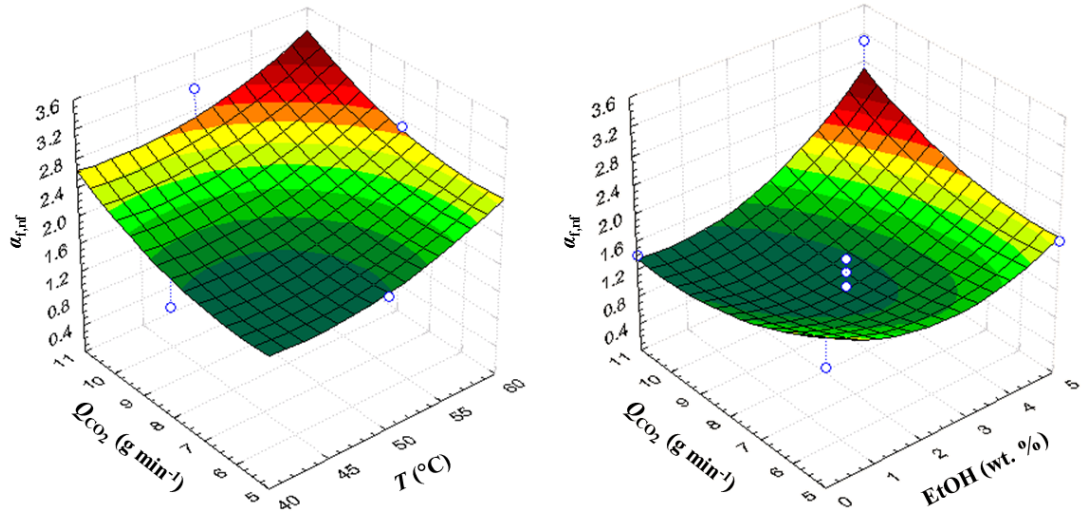

Figure 5 – Response surface plotting the effects of (a) temperature and carbon dioxide flow rate on selectivity to friedelin for 5 wt.% EtOH content and (b) ethanol content and carbon dioxide flow rate on selectivity to friedelin at 50℃ (reduced model). Dots are experimental data and surface is given by Eq. (12)

3.2 Experiments at optimal operating conditions

The fitted reduced models were used to search optimum operating conditions to maximize the respective response, being these results presented in Table 5. With reference to η_{Total}, the optimum was found for maximum values of temperature (60 °C), ethanol content (5 wt.%) and a CO_2 flow rate (11 g min^{-1}), which is a set of conditions not measured in the original experimental plan of the Box-Behnken design. Under these conditions, the predicted total extraction yield (according to Eq. 8) is 2.2 wt.%, with the other two responses - $C_{\mathrm{Friedelin}}$ and $\alpha_{\mathrm{F,nF}}$ - scoring 36.0 wt.% and 3.3, respectively. Remarkably, the optimum conditions for η_{Total} coincide in our case with the optimum conditions for an enhanced selectivity towards friedelin. This is an interesting occurrence, in the sense that $\alpha_{\mathrm{f,nf}}$ is much rarely computed in SFE studies, and optimization is many times driven only by the bulk extract production, i.e. η_{Total}.

In turn, the preferable operating conditions for a maximized $C_{\mathrm{Friedelin}}$ are considerably distinct, pointing to 40 °C, 0 wt.% and 5 g min^{-1}. Under these conditions, friedelin content in the extracts is 38.2 wt.%, which is only 1.06 times higher than the value obtained under the optimum conditions for the other responses. In addition, η_{Total} exhibits a decrease of 78.2 % (under $C_{\mathrm{Friedelin}}$ optimum conditions) in relation to its own optimum, and the predicted selectivity is 0.84 times lower. Hence, despite the preference to operate at a lower temperature (40 ºC) and without cosolvent, the optimum conditions for $C_{\mathrm{Friedelin}}$ impose a too heavy penalty on total yield for just an incremental gain of 2.2 % in friedelin concentration in the resulting extract. For this reason, we chose to accomplish an experimental confirmation of the predicted optima for the conditions corresponding to the maximum values of both η_{Total} and $\alpha_{\mathrm{F,nF}}$.

Table 5 - Optimum conditions for each response and predicted response values under these conditions.

		η_{Total} (wt.%)	$C_{\mathrm{Friedelin}}$ (wt. %)	$\alpha_{\mathrm{F,nF}}$
Optimum Conditions	T (°C)	60	40	60
	EtOH (wt. %)	5	0	5
	Q_{CO_2} (g min^{-1})	11	5	11
η_{Total} (wt.%)		**2.2**	0.48	2.2
$C_{\mathrm{Friedelin}}$ (wt. %)		36.0	**38.2**	36.0
$\alpha_{\mathrm{F,nF}}$		3.3	2.8	**3.3**

By performing an additional experimental assay under the optimum conditions of η_{Total} and $\alpha_{\mathrm{F,nF}}$ (SFE16: 60 ºC/ 5 wt.%/ 11 g min^{-1}), a total extraction yield of 2.4 wt.% was obtained, which is the higher than the predicted one (2.2 wt.%). Additionally, such value is the highest within the experimental space studied, thus confirming the success of the model prediction. Also, the underestimation of the model at the optimum conditions is in agreement with a previously observed underrating tendency of the response surface in that experimental region (see Figure 3a). In turn, the attained $\alpha_{\mathrm{F,nF}}$ scored 1.7, which is 48.4 % lower than the predicted value. Lastly the experimental value of $C_{\mathrm{Friedelin}}$ in SFE16 was 27.4, being much lower than the prediction of the model for that response.

As a supplementary study, an additional assay (SFE17) was performed with four times more cosolvent than SFE16 (and keeping all the other operating conditions of SFE16), with the goal of testing even further the impact of cosolvent addition in the extraction results. Accordingly, an experimental total extraction yield of 4.6 wt.% was attained, being represented in Figure 6 altogether with runs SFE16 (the optimum conditions according to η_{Total} and $\alpha_{\mathrm{F,nF}}$ RSM surfaces) and with SFE11 and SFE15 (the highest experimental η_{Total} values obtained in the Box-Behnken design plan). Remarkably, the SFE17 results, overcome the η_{Total} of SFE16 by 52 % , and corresponds to 1.07 times the reference dichloromethane yield obtained with Soxhlet.

In Figure 7 friedelin concentration in the extracts is plotted for the same assays. It can be seen that the optimal operating conditions SFE16 led to a decrease in terms of friedelin content to 27.4 wt.% which lies within the lowest $C_{\mathrm{Friedelin}}$ values obtained in the original Box-Behnken design plan. Moreover, it is also important to highlight the even lower friedelin concentration obtained in the additional assay with 20 wt.% of ethanol, scoring 22.2 wt.%. Remarkably, while this behavior emphasizes the high affinity of ethanol to coextract polar compounds (such as phenolic compounds or sugars), the specific friedelin yield - computable by the product $\eta_{\mathrm{Total}} \times C_{\mathrm{Friedelin}}$ - shows that SFE17 was able to remove 1.02 wt.% of friedelin from the biomass, while SFE16 achieved only 0.66 wt%. This means that a four times greater cosolvent content was able to almost duplicate total extraction yield, and to increase friedelin removal from the cork matrix by 55 %.

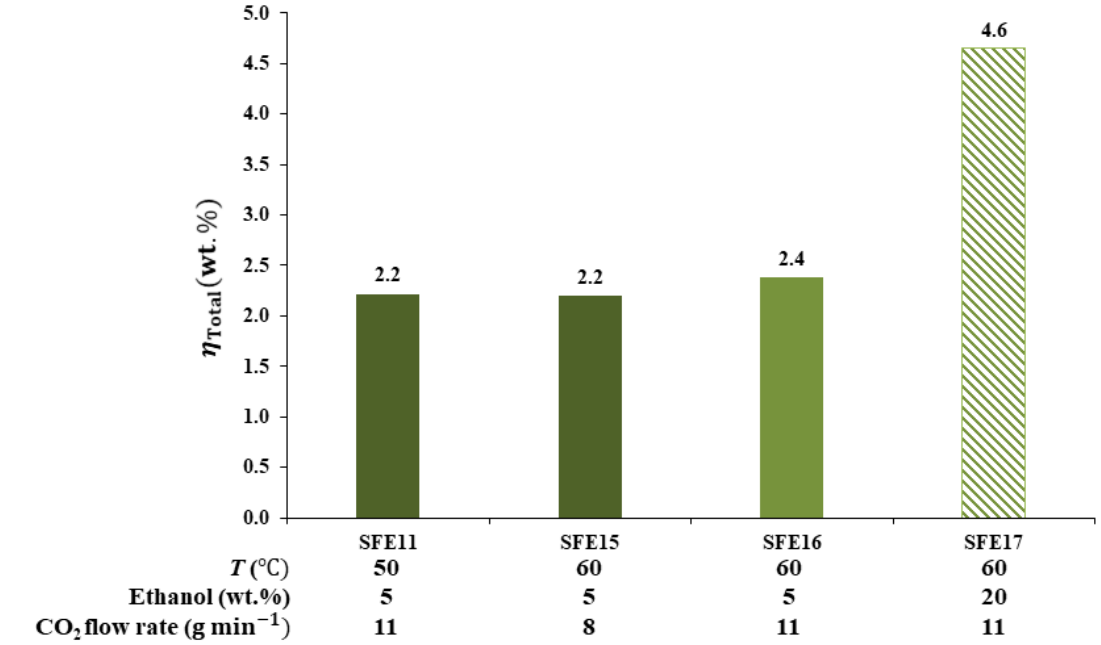

Figure 6 – Experimental total extraction yield for predicted optimum operating conditions (SFE16), and for an additional assays with 20 wt.% of EtOH. Data from the original Box-Behnken design plan (SFE11 and SFE15) are plotted for comparison.

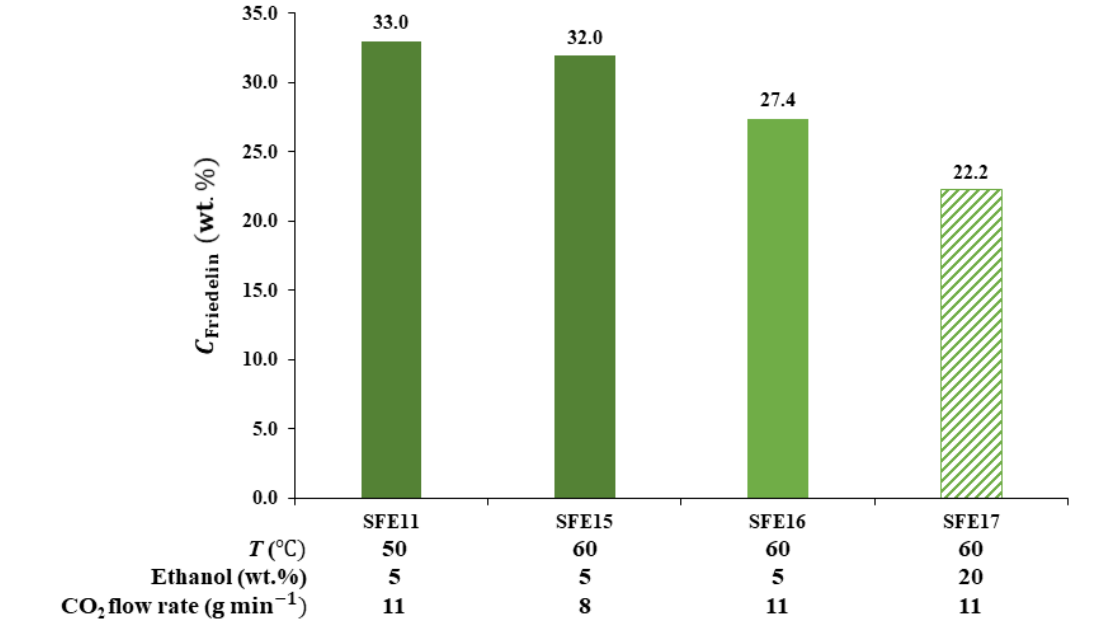

Figure 7 – Experimental friedelin concentration for predicted optimum operating conditions (SFE16), and for an additional assays with 20 wt.% of EtOH. Data from the original Box-Behnken design plan (SFE11 and SFE15) are plotted for comparison.

3.3 Validation tests

For model validation, available experimental η_{Total} and $C_{\mathrm{Friedelin}}$ data from previous studies with the same biomass [11] and from previous chapter are presented in Table 6 together with the predicted values obtaining with the fitted surface models developed in this work, plus the respective absolute relative deviations (AARDs). Moreover, $\alpha_{\mathrm{F,nF}}$ values were calculated for the selected literature assays and added to enable validation of the model on that response as well.

Regarding the results obtained for total extraction yield, it is possible to say that the model provided good estimates of the experimental data despite being lower than those obtained experimentally (as previously discussed). Accordingly, the resulting AARD was 10.3 %, scoring below the original AARD of the model fitting that amounted 11.1 %. Hence, these results confirm the good prediction capacity of the η_{Total} model. Moreover, in Figure 8, the predicted η_{Total} of the validation assays are plotted against the experimental η_{Total} values, and all the predicted vs. experimental η_{Total} values of the Box-Behnken design plan are also graphed. As a first insight, the random distribution of the points around the diagonal is visible for the fitted data, which validates the randomness of the validation test points. Secondly, the particular overestimation at the validation tests is depicted. Finally, the lower AARD of the validation data set is also perceived through a greater closeness to the diagonal in relation to the data used to create the regression model.

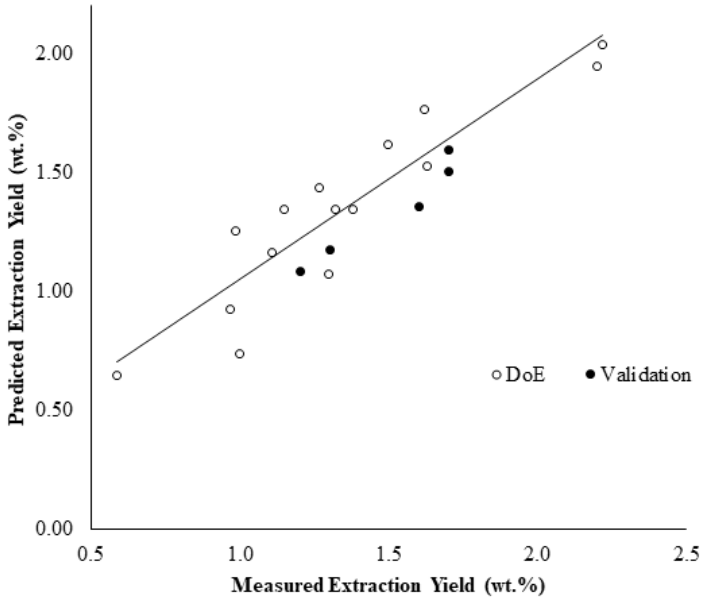

Figure 8 – Predicted versus measured total extraction yield (wt.%) for the Design of Experiments (DoE) and validation tests.

For the friedelin concentration response, the validation AARD reached 15.8 %, and highly contrasts with the AARD value of 4.1 % attained for the original RSM model. This model exhibited a weaker prediction capacity and a tendency to overestimate $C_{\mathrm{Friedelin}}$ values. In turn, a severer prediction fragility was revealed by $\alpha_{\mathrm{F,nF}}$ model in the validation test. While the original RSM model had AARD of 12.2 %, the model exhibited a deviation of 33.1 % when applied to the validation assays. In practice, this translates into a tendency to overestimate the selectivities, namely by predicting values between 1.6 and 1.9 while in practice they scored between 1.1 and 1.5.

On the whole, the validation tests point to a good robustness of η_{Total} response, and to more dubious performances regarding $C_{\mathrm{Friedelin}}$ and $\alpha_{\mathrm{F,nF}}$ responses.

Table 6 – Experimental results from previous chapter and from literature [11], and predicted results for model validation.

Run	T (℃)	EtOH (wt.%)	Q_{CO_2} (g min^{-1})	η_{Total} (wt. %)		$C_{Friedelin}$ (wt. %)		$\alpha_{F,nF}$	
				Predict (Eq. (10))	Exp	Predict (Eq. (11))	Exp	Predict (Eq. (12))	Exp
SFE18[a]	40	2.5	8	1.2	1.3	30.5	25.1	1.6	1.1
SFE19[a]	40	5.0	5	1.4	1.6	34.9	25.2	1.9	1.1
SFE20[a]	50	2.5	5	1.1	1.2	28.9	28.5	1.6	1.4
SFE21[a]	60	2.5	8	1.5	1.7	28.5	28.3	1.6	1.5
SFE22[b]	50	2.5	11	1.6	1.7	28.9	24.7	1.6	1.1
			Validation AARD (%)	-	10.3	-	15.8	-	33.1
			Original RSM model AARD (%)	11.1	-	4.1	-	12.2	-

[a] Retrieved from previous chapter; [b] retrieved from [11].

4. Conclusions

The optimization of the supercritical fluid extraction of *Quercus cerris* cork was carried out for three process variables: temperature (40-60 ℃), cosolvent content (ethanol, 0-5 wt.%) and CO_2 flow rate (5-11 g min^{-1}) using Box-Behnken design of experiments and response surface methodology. The studied responses were total extraction yield, friedelin concentration and selectivity to friedelin.

For the experimental space considered, the maximum total extraction yield (η_{Total} = 2.2 wt.%) was attained in runs SFE11 (50 ℃, 5.0 wt.% EtOH, 11 g min^{-1}) and SFE15 (60 ℃, 5.0 wt.% EtOH, 8 g min^{-1}). In this response, Pareto chart showed that the linear effect of EtOH is by far the most influent operating condition. Then increases of the CO_2 flow rate induce a slightly stronger impacts in η_{Total} when compared with temperature. While of lower rank, a positive impact of temperature was observed, implying that vapor pressure increase prevailed (in general) over density reduction. Moreover, the model points a maximum value of η_{Total} (2.2 wt.%) for the maximum values of T (60 ℃), ethanol content (5 wt.%) and a CO_2 flow rate (11 g min^{-1}).

For friedelin concentration ($C_{Friedelin}$), the values ranged from 25.3 wt.% in run SFE7 (50 ℃, 2.5 wt.% EtOH, 8 g min^{-1}) to 36.2 wt. % in run SFE2 (40 ℃, 2.5 wt.% EtOH, 5 g min^{-1}). The respective maximum of $C_{Friedelin}$ in *Q. cerris* extracts ($C_{Friedelin}$= 38.2 wt.%) are the combination of a lower temperature (40 ℃) with no cosolvent addition (0 wt.% EtOH) and lower CO_2 flow rate (5 g min^{-1}).

The experimental $\alpha_{F,nF}$ values ranged from 1.1 in run SFE7 (50 ℃, 2.5 wt.% EtOH, 8 g min^{-1}) to 3.1 in run SFE11 (50 ℃, 5 wt.% EtOH, 11 g min^{-1}). It is important to highlight that all of the attained selectivity values were higher than 1.0, so one can expect friedelin to be removed selectively over all the other compounds within the operating conditions studied. The reduced model predicts that the highest selectivity to friedelin to be $\alpha_{F,nF}$ = 3.3 (at t = 8.0 h), and that it can be obtained at the highest levels of each studied factor, i.e. 60 ℃, 5 wt.% EtOH, and 11 g min^{-1}.

The optimum conditions for η_{Total} coincide in our case with the optimum conditions for an enhanced selectivity to friedelin. In turn, the preferable operating conditions for a maximized $C_{Friedelin}$ are considerably distinct and impose a too heavy penalty on total yield for just an incremental gain of 2.2 % in the friedelin concentration in the resulting extract. Furthermore, an additional assay was performed with four times more cosolvent (i.e. 20 wt.%) and an experimental total extraction yield of 4.6 wt.%

was attained. This value overcame the η_{Total} of optimum conditions by 52 %. Howver, a lower friedelin concentration was obtained in the additional assay, scoring 22.2 wt.%.In turn, validation tests were performed for the fitted models, and a better robustness was verified for the η_{Total} response, in contrast to the performances of $C_{\mathrm{Friedelin}}$ and $\alpha_{\mathrm{F,nF}}$ responses.

On the whole, the reported study emphasized how the most aggressive operating conditions do not always lead to the best results, particularly those that depend on specific chemical trade-offs and not on intensity. In fact, the optimal conditions depend in what is the main goal of extraction: an extract enriched in a higher diversity of compounds (higher total extraction yield) or in a target compound like friedelin.

5. References

[1] S. Silva, M. Sabino, E. Fernandes, V. Correlo, L. Boesel, and R. L. Reis, "Cork: properties, capabilities and applications (vol 50, pg 345, 2005)," *Int. Mater. Rev.*, vol. 53, p. 256, Jul. 2008.

[2] H. Pereira, *Cork: Biology, Production and Uses*. 2007.

[3] C. B. Lopes *et al.*, "Cork stoppers as an effective sorbent for water treatment: The removal of mercury at environmentally relevant concentrations and conditions," *Environ. Sci. Pollut. Res.*, vol. 21, no. 3, pp. 2108–2121, 2014.

[4] S. Silva, M. Sabino, E. Fernandes, V. Correlo, L. Boesel, and R. L. Reis, "Cork: properties, capabilities and applications (vol 50, pg 345, 2005)," *Int. Mater. Rev.*, vol. 53, p. 256, Jul. 2008.

[5] I. M. Aroso, A. R. Araújo, R. A. Pires, and R. L. Reis, "Cork: Current Technological Developments and Future Perspectives for this Natural, Renewable, and Sustainable Material," *ACS Sustain. Chem. Eng.*, vol. 5, no. 12, pp. 11130–11146, 2017.

[6] A. Şen, M. M. R. De Melo, A. J. D. Silvestre, H. Pereira, and C. M. Silva, "Prospective pathway for a green and enhanced friedelin production through

supercritical fluid extraction of *Quercus cerris* cork," *J. Supercrit. Fluids*, vol. 97, pp. 247–255, 2015.

[7] C. Sunil, V. Duraipandiyan, S. Ignacimuthu, and N. A. Al-Dhabi, "Antioxidant, free radical scavenging and liver protective effects of friedelin isolated from *Azima tetracantha Lam.* leaves," *Food Chem.*, vol. 139, no. 1–4, pp. 860–865, 2013.

[8] P. Antonisamy, V. Duraipandiyan, and S. Ignacimuthu, "Anti-inflammatory, analgesic and antipyretic effects of friedelin isolated from *Azima tetracantha Lam.* in mouse and rat models," *J. Pharm. Pharmacol.*, vol. 63, no. 8, pp. 1070–1077, 2011.

[9] B. Lu, L. Liu, X. Zhen, X. Wu, and Y. Zhang, "Anti-tumor activity of triterpenoid-rich extract from bamboo shavings (*Caulis bamfusae* in Taeniam)," vol. 9, no. 38, pp. 6430–6436, 2010.

[10] R. A. R. Pires, S. P. A. S. . Martins, J. A. M. Chagas, and R. L. G. Reis, "Extraction and purification of friedelin," EP2070906A1.

[11] M. M. R. de Melo, A. Şen, A. J. D. Silvestre, H. Pereira, and C. M. Silva, "Experimental and modeling study of supercritical CO_2 extraction of *Quercus cerris cork:* Influence of ethanol and particle size on extraction kinetics and selectivity to friedelin," *Sep. Purif. Technol.*, vol. 187, pp. 34–45, 2017.

[12] M. M. R. De Melo, A. J. D. Silvestre, and C. M. Silva, "Supercritical fluid extraction of vegetable matrices: Applications, trends and future perspectives of a convincing green technology," *J. Supercrit. Fluids*, vol. 92, pp. 115–176, 2014.

[13] H. M. A. Barbosa, M. M. R. De Melo, M. A. Coimbra, C. P. Passos, and C. M. Silva, "Optimization of the supercritical fluid coextraction of oil and diterpenes from spent coffee grounds using experimental design and response surface

methodology," *J. Supercrit. Fluids*, vol. 85, pp. 165–172, 2014.

[14] C. Da Porto, D. Voinovich, D. Decorti, and A. Natolino, "Response surface optimization of hemp seed (*Cannabis sativa L.*) oil yield and oxidation stability by supercritical carbon dioxide extraction," *J. Supercrit. Fluids*, vol. 68, pp. 45–51, 2012.

[15] R. M. A. Domingues, M. M. R. De Melo, E. L. G. Oliveira, C. P. Neto, A. J. D. Silvestre, and C. M. Silva, "Optimization of the supercritical fluid extraction of triterpenic acids from *Eucalyptus globulus* bark using experimental design," *J. Supercrit. Fluids*, vol. 74, pp. 105–114, 2013.

[16] K. Zaghdoudi *et al.*, "Response surface methodology applied to Supercritical Fluid Extraction (SFE) of carotenoids from Persimmon (*Diospyros kaki L.*)," *Food Chem.*, vol. 208, pp. 209–219, Oct. 2016.

[17] V. H. Rodrigues, M. M. R. de Melo, I. Portugal, and C. M. Silva, "Extraction of *Eucalyptus* leaves using solvents of distinct polarity. Cluster analysis and extracts characterization," *J. Supercrit. Fluids*, vol. 135, no. January, pp. 263–274, 2018.

[18] D. Bas and I. H. Boyaci, "Modeling and optimization I: Usability of response surface methodology," *J. Food Eng.*, vol. 78, no. 3, pp. 836–845, 2007.

[19] D. C. Montgomery, *Design and Analysis of Experiments*. USA: John Wiley & Sons, Inc., 2006.

[20] M. M. R. de Melo, E. L. G. Oliveira, A. J. D. Silvestre, and C. M. Silva, "Supercritical fluid extraction of triterpenic acids from *Eucalyptus globulus* bark," *J. Supercrit. Fluids*, vol. 70, pp. 137–145, Oct. 2012.

IV. Final conclusions and future work

The present work aimed to study the potential of *Quercus cerris* cork as a source of extracts rich in bioactive compounds, namely friedelin, a pentacyclic triterpene ketone. Accordingly, Soxhlet and batch solid-liquid extractions (SLE) were carried out with methanol, ethanol, dichloromethane and petroleum ether, as well as supercritical fluid extraction (SFE) using modified carbon dioxide. FTIR-ATR and GC-MS techniques were used to characterize the obtained extracts, and multidimensional scaling analysis (MDS) was employed to efficiently compare them. An experimental optimization of the SFE was performed for three process variables: temperature (40-60 ℃), cosolvent content (0-5 wt.% of ethanol), and CO_2 flow rate (5-11 g min^{-1}). For this, a Box-Behnken design of experiments and response surface methodology were applied. The studied responses were total extraction yield (η_{Total}), friedelin concentration ($C_{\mathrm{Friedelin}}$) and the extraction selectivity towards friedelin ($\alpha_{\mathrm{F,nF}}$).

Within the studied extractions methods, the maximum total extraction yield was attained for the Soxhlet extraction with methanol (η_{Total} = 13.8 wt.%) and the minimum was attained by batch SLE with petroleum ether (η_{Total} = 0.35 wt.%). A significant variability of η_{Total} values was noticed, marked by the higher yields being obtained with polar solvents, namely methanol and ethanol. Accordingly, the FTIR-ATR spectra of the extracts highlight the affinity of methanol and ethanol to remove high polar compounds in comparison with dichloromethane, petroleum ether and also supercritical CO_2. For the supercritical fluid extractions, η_{Total} ranged from 1.2 wt.% for run SFE3 (50 ℃, 2.5 wt.% EtOH, 5 g min^{-1}) to 1.7 wt.% for run SFE4 (60 ℃, 2.5 wt.% EtOH, 8 g min^{-1}). In addition, a positive impact of temperature and cosolvent in SFE was also notorious, being the greatest yields obtained with higher ethanol content or at the highest temperature. For friedelin concentration, the results ranged from 41.3 wt. % (Soxhlet with dichloromethane) to 5.4 wt. % (batch SLE with methanol). The best performing assays in terms of $C_{\mathrm{Friedelin}}$ were those involving weakly/non-polar solvents. Batch extractions reached $C_{\mathrm{Friedelin}}$ values significantly lower than Soxhlet extractions with the same solvent, which reinforces the influence of temperature and pure solvent on the friedelin uptake. The SFE assays provided $C_{\mathrm{Friedelin}}$ results better than most Soxhlet and batch SLE experiments, which confirms the interesting selectivity to friedelin of that method.

For the experimental optimization of SFE of *Q. cerris* cork, the conditions that maximize η_{Total} (2.2 wt.%) and $\alpha_{\mathrm{F,nF}}$ (3.3 at, t = 8.0 h) were the maximum values of T (60 ºC), ethanol content (5 wt.%) and a CO_2 flow rate (11 g min^{-1}). In fact, all of the attained selectivity values were higher than 1.0, so one can expect friedelin to be removed selectively over all the other compounds within the operating conditions studied.

For friedelin content in the extracts, the maximum ($C_{\mathrm{Friedelin}}$= 38.2 wt.%) was attained for the combination of low temperature (40 ℃), no cosolvent (0 wt.% EtOH) and low CO_2 flow rate (5 g min^{-1}). Nonetheless, the preferable operating conditions for a maximized $C_{\mathrm{Friedelin}}$ impose a too heavy penalty on total yield for just an incremental gain of 2.2 % in the resulting extract. The optimal conditions depend on what is the main goal of extraction: an extract enriched in a higher diversity of compounds (higher total extraction yield) or in a target compound like friedelin. Actually, this idea can be extended to all extraction methods and solvents, as disclosed by the multidimensional scaling analysis.

On the whole, this thesis provides strong arguments towards the production of friedelin enriched extracts from *Quercus cerris* cork through SFE technology, under the biorefinery concept.

As future work possibilities, the produced extracts can be tested and further optimized towards the specificities of the application fields where a bioactive compound like friedelin can be deemed valuable. In this context, features such as antioxidant, anti-inflammatory and anti-tumor activity can be checked for the produced extracts. In addition, purification processes for friedelin can be designed and applied to the already enriched extracts, making it a promising investigation pathway for applications demanding isolated bioactive compounds. As per the SFE process, upcoming steps might comprise the realization of *scale-up* studies and/or the accomplishment of a techno-economic analysis of the process in order to estimate the expectable costs of the extracts under industrial scenarios.